University of South Bohemia

Faculty of Science

Functional analysis of Salp25D, a homologue of peroxiredoxin, from castor bean tick *Ixodes ricinus*

MASTER THESIS

Bc. Radka Hobizalová, BSc.

Supervisor: Nataliia Rudenko, PhD.

Co-supervisor: Maryna Golovchenko, MSc.

Faculty guarantee: Prof. RNDr. Libor Grubhoffer, CSc.

České Budějovice, 2012

Hobizalova, R., 2012: Functional analysis of Salp25D, a homologue of peroxiredoxin, from castor bean tick *Ixodes ricinus.* Mgr. Thesis, in English – 64 p., Faculty of Science, University of South Bohemia, České Budějovice, Czech Republic.

Annotation:
Antioxidant enzymes play an important role in detoxification of reactive oxygen species, thus protecting the organism from oxidative damage. The blood-feeding lifestyle of ticks is a source of oxidative stress that needs to be balanced by an appropriate antioxidant defense. In this study, a homologue of one-cysteine peroxiredoxins named Salp25D from the tick *I. ricinus* is described, and its antioxidant activity *in vitro* is confirmed. Due to similarity with protein from *I. scapularis*, it is assumed that *I. ricinus* Salp25D might be involved in processes at tick-host-pathogen interface, facilitating acquisition and potentially also transmission of *B. burgdorferi* spirochetes.

Financial sources: GAČR P302/11/3133

I hereby declare that I have worked on my master thesis independently and used only the sources listed in the bibliography.

I hereby declare that, in accordance with Article 47b of Act No. 111/1998 in the valid wording, I agree with the publication of my master thesis, in full to be kept in the Faculty of Science archive, in electronic form in publicly accessible part of the STAG database operated by the University of South Bohemia in České Budějovice accessible through its web pages. Further, I agree to the electronic publication of the comments of my supervisor and thesis opponents and the record of the proceedings and results of the thesis defense in accordance with aforementioned Act No. 111/1998. I also agree to the comparison of the text of my thesis with the Theses.cz thesis database operated by the National Registry of University Theses and a plagiarism detection system.

Date:
Signature:

Acknowledgement:

I would like to thank Professor Libor Grubhoffer for giving me the opportunity to work in his laboratory. Further, my thanks go to my supervisors, Natasha Rudenko and Maryna Golovchenko for their scientific guidance. They were always willing to help and answer my questions. Thanks go to our lab group members, for creating a nice atmosphere in the lab as well as for their valuable advice, and to the people from the neighboring labs, namely Gábina Loosová and Ondra Hajdušek, Martina Kovářová, Helča Langhansová and Radek Šíma, for their help with specialized methods. Last, but not least, I would like to thank my boyfriend Martin for standing by me all the time, and my parents for supporting me throughout my whole studies.

LIST OF ABBREVIATIONS

1-Cys Prx - one cysteine peroxiredoxin
2-Cys Prx - two cysteine peroxiredoxin
AA – amino acid
CAT - catalase
cDNA - complementary DNA
FACS - fluorescence activated cell sorting
G - gut
GFP - green fluorescent protein
GPx - glutathine peroxidase
GR - glutathione reductase
Grx - glutaredoxin
GSH/ GSSG - reduced/oxidized glutathione
MCO - metal catalyzed oxidation
NADPH/$NADP^+$ - reduced/oxidized nicotinamide adenine dinucleotide phosphate
OV - ovaries
PCR - polymerase chain reaction
PMA - phorbol 12-myristate 13-acetate
Prx – peroxiredoxin
qRT-PCR - quantitative reverse transcription-polymerase chain reaction
RNAi - RNA interference
ROS - reactive oxygen species
rSalp25D - recombinant salivary protein (mass 25kDa)
rxn - reaction
SAT - saliva activated transmission
SDS-PAGE - sodium dodecylsulphate - polyacrylamide gel electrophoresis
SG - salivary glands
SGE - salivary gland extract
SOD - superoxide dimutase
ssRNA/dsRNA - single-stranded/double-stranded RNA
Trx - thioredoxin
TrxR - thioredoxin reductase

TABLE OF CONTENTS

1 INTRODUCTION 1

1.1 Reactive oxygen species (ROS) and oxidative stress 1

1.1.1 Sources of ROS 2
1.1.2 ROS-induced oxidative damage 2

1.2 Antioxidant defense 3

1.2.1 Non-enzymatic antioxidants 3
1.2.2 Enzymatic antioxidants 4

1.2.2.1 Catalase (CAT) 4
1.2.2.2 Superoxide dismutase (SOD) 4
1.2.2.3 Glutathione peroxidase (GPx) 5
1.2.2.4 Peroxiredoxin (Prx, Prdx) 6
1.2.2.5 Thioredoxin and glutathione/glutaredoxin systems 11

1.3 Ticks 12
1.4 Oxidative stress and antioxidant defense in ticks 13

1.4.1 Blood digestion-induced oxidative stress 14
1.4.2 Oxidative stress within tick-host interface 16

1.5 Anti-tick vaccines 19
1.6 Salp25D from *Ixodes ricinus* 20

2 GOALS OF THE WORK 22
3 MATERIALS 23

3.1 Chemicals, buffers, media 23
3.2 Kits 27
3.3 Primers 27
3.4 Ticks 27

4 METHODS 28

4.1 Bioinformatic analysis 28
4.2 Verification of Salp25D insert in the expression vector 28
4.3 Production of recombinant protein in a bacterial system 28

4.3.1 Transformation of competent *E. coli* cells with the expression vector 28
4.3.2 Pilot expression – time course monitoring 28
4.3.3 Optimization of induction temperature 29
4.3.4 Large-scale expression of Salp25D 29

4.4 Purification of recombinant protein 29

4.4.1 Preparation of *E. coli* lysate 29
4.4.2 Purification on Ni-NTA column 29

4.5 SDS-PAGE analysis 30
4.6 Dialysis, concentration 30
4.7 Western blotting 30
4.8 Functional assays 30

4.8.1 DNA nicking assay 30

4.8.2 Borrelia viability assay – LIVE/DEAD 31
4.8.3 Borrelia viability assay – FACS 32
4.8.4 Assay for glutathione peroxidase (GPx) activity 32
4.9 RNA interference 33
4.9.1 Preparation of dsRNA 33
4.9.1.1 PCR with primers for RNAi 33
4.9.1.2 Restriction of PCR product and plasmid pLL10 33
4.9.1.3 Ligation into pLL10 vector 33
4.9.1.4 Transformation, selection of positive clones 34
4.9.1.5 Restriction of purified plasmid 34
4.9.1.6 Purification of digested plasmid 35
4.9.1.7 Synthesis of ssRNA (in vitro transcription) 35
4.9.1.8 Synthesis of dsRNA 35
4.9.2 Tick injection 36
4.9.3 Tick feeding and dissection 36
4.9.4 Confirmation of gene silencing 36
4.9.4.1 Total RNA isolation 36
4.9.4.2 cDNA synthesis 36
4.9.4.3 Quantitative PCR 37
5 RESULTS 38
5.1 Bioinformatic analysis 38
5.2 Salp25D insert in the expression vector 38
5.3 Production of recombinant protein in a bacterial system 39
5.3.1 Pilot expression – time course monitoring, temperature optimization 39
5.3.2 Protein purification 39
5.3.3 Western blot 40
5.4 Functional assays 41
5.4.1 DNA nicking assay 41
5.4.2 Borrelia viability assay – LIVE/DEAD 41
5.4.3 Borrelia viability assay – FACS 42
5.4.4 Assay for GPx activity 43
5.5 RNA interference 45
5.5.1 dsRNA preparation 45
5.5.2 Tick injection and feeding 46
5.5.3 Salp25D silencing 47
6 DISCUSSION AND CONCLUSIONS 49
7 BIBLIOGRAPHY 53
8 APPENDIX 63

1 INTRODUCTION

1.1 Reactive oxygen species (ROS) and oxidative stress

The term reactive oxygen species (ROS) is used to describe a set of oxygen-containing reactive molecules and free radicals. Molecules that can be classified as ROS are hydrogen peroxide (H_2O_2), organic hydroperoxides (ROOH), superoxide ($O_2^{\bullet-}$), hydroxyl ($OH^{\bullet}$) and hydroperoxyl radicals ($OOH^{\bullet}$), or hypochlorite ion (OCl^-). Although they may play important roles in cellular signaling (*1*) and pathogen killing (*2*), they are also implicated in damage of key biomolecules such as lipids, nucleic acids or proteins. At normal physiological levels, ROS are detoxified by several antioxidant molecules. In the other case, accumulation of ROS in the organism leads to redox imbalance and a condition known as oxidative stress (*3*). Oxidative stress has already been implicated in many pathological processes and diseases (*2*).

ROS can interconvert between each other (reactions 1-3). Superoxide radical is a primary ROS in terms of production in the organism. It is usually dismutated to yield H_2O_2. Hydrogen peroxide is not a radical species, but it serves as pro-oxidant molecule (*4*). It has lower reactivity in comparison to other ROS, making it an ideal candidate for cell signaling function (*1*). It can be reduced to hydroxyl radicals via metal ion catalyzed reaction (reactions 4-6). Hydroxyl radical is an extremely reactive species and is therefore responsible for majority of deleterious effects caused by ROS. It can promote further formation of various organic radicals (reactions 7-10).

1. $O_2 + e^- \rightarrow \mathbf{O_2^{\bullet-}}$ superoxide radical
2. $O_2^{\bullet-} + e^- \rightarrow O_2^{2-} + 2H^+ \rightarrow \mathbf{H_2O_2}$ hydrogen peroxide
3. $H_2O_2 + e^- \rightarrow \mathbf{OH^{\bullet}} + OH^-$ hydroxyl radical

4. $O_2^{\bullet-} + Fe^{3+} \rightarrow Fe^{2+} + O_2$
5. $H_2O_2 + Fe^{2+} \rightarrow Fe^{3+} + OH^{\bullet} + OH^-$ Fenton reaction
6. sum: $H_2O_2 + O_2^{\bullet-} \rightarrow OH^{\bullet} + OH^- + O_2$ Haber-Weiss reaction

7. $R - H + OH^{\bullet} \rightarrow \mathbf{R^{\bullet}} + H_2O$ alkyl radical
8. $R^{\bullet} + O_2 \rightarrow \mathbf{ROO^{\bullet}}$ peroxyl radical
9. $ROO^{\bullet} + R - H \rightarrow \mathbf{ROOH} + R^{\bullet}$ alkyl hydroperoxide
10. $ROOH + Fe^{2+} \rightarrow \mathbf{RO^{\bullet}} + OH^- + Fe^{3+}$ alkoxyl radical

1.1.1 Sources of ROS

Endogenous sources

Majority of ROS in the organism are generated by aerobic metabolism. The mitochondrial respiratory chain is responsible for processing molecular oxygen to water, but can also yield superoxide radicals as an undesired product. It happens mainly in complex I and III of the electron transport chain. Mitochondria deal with the situation by converting $O_2^{\bullet-}$ to H_2O_2 by the action of superoxide dismutase (*5*, *6*).

Some redox enzymes are sources of ROS as well. NADPH oxidase present in phagocytic cells is known to produce $O_2^{\bullet-}$ as a part of pathogen-killing mechanism (*7*). Xanthine oxidase is responsible for production of $O_2^{\bullet-}$ and NO, which together create a potent oxidant – peroxinitrite (*8*). Peroxisomal oxidases produce H_2O_2 during the metabolism of other substances. Among other enzymes generating ROS, nitric oxide synthase, 5-lipoxygenase or cytochrome P450 should be also mentioned (*4*).

Exogenous sources

Environmental factors, such as the exposition to heavy metals, chlorinated compounds or ionizing and UV radiation, contribute to oxidative stress (*3*) as well as treatment with particular xenobiotics (*9*).

1.1.2 ROS-induced oxidative damage

DNA oxidation

Of the reactive oxygen species, the hydroxyl radicals react with DNA and cause its modifications. These include changes in DNA bases, sugar moieties, single- and double-stranded breaks or DNA cross-links (*3*). Reaction of $OH^{\bullet}$ with purines and pyrimidines give rise to various base lesions. A molecule of 8-oxo-2′deoxyguanosine is the one of the most studied and has been already established as the marker of oxidative stress (*10*). Some of the base lesions were reported to be mutagenic, causing *in situ* base substitutions or base misincorporations (*11*), affecting the replication and transcription process (*10*).

Lipid peroxidation

Membrane lipids are vulnerable to oxidative damage due to high content of polyunsaturated fatty acids (*3*). The process of lipid peroxidation is a typical example of radical chain reaction. It is initiated by $OH^{\bullet}$ and proceed through fatty acid peroxyl radical ($LOO^{\bullet}$) to lipid

hydroperoxides (LOOH) and cyclic forms of those (*12*). Unstable LOOH generate new peroxyl and alkoxyl ($LO^{\bullet}$) radicals and decompose to secondary products, including aldehydes. These often serve as oxidative stress biomarkers (*13*). An example is malondialdehyde which reacts with DNA bases to form mutagenic DNA adducts (*14*). Other major end-product, 4-hydroxy-2-nonenal, serves as signal mediator at physiological levels, but is toxic at high concentrations (*3*).

Protein oxidation

Hydroxyl radicals produced via ionizing radiation or through Fenton chemistry cause protein damage at various levels. First of all, protein backbone may be cleaved by the action of $OH^{\bullet}$ or derived alkoxyl radicals. Amino acid side chains are also prone to oxidation (especially Arg, Cys, Glu, His, Lys, Met, Phe, Pro, Thr, Trp, Tyr and Val) yielding various products, often carrying a carbonyl group. Another type of protein modification are protein cross-links, created either by the interaction of carbon-centered radicals, oxidized Cys (→ disulfide cross-link) and Tyr (→ dityrosine cross-link) residues, or addition of certain amino acid side chains to formerly oxidized products (*15*). Proteins can be also damaged indirectly, by the oxidation of lipids and carbohydrates and subsequent formation of carbonyl-protein adducts (*16*). All these changes may partially destroy secondary or tertiary protein structure, thus being responsible for the loss of enzymatic activity or altered cell function (*12*, *16*).

1.2 Antioxidant defense

Organisms use multiple strategies to fight the oxidative stress. There is a variety of small molecules, but also larger enzymes or enzyme systems that act as antioxidants. Together, they prevent DNA, proteins and lipids from the damage by reactive oxygen species (*3*).

1.2.1 Non-enzymatic antioxidants

Non-enzymatic antioxidants are usually small molecules that function as radical scavengers. Often, they are also able to regenerate other antioxidants within the antioxidant network. Some of them work in the aqueous environment of cell cytosol (glutathione, ascorbic acid/vitamin C, uric acid, flavonoids), whereas the other prefer hydrophobic conditions of lipid membranes (α-tocopherol/vitamin E, caroteinoids, ubiquinone). Few of them operate in both environments (α-lipoic acid) (*3*).

1.2.2 Enzymatic antioxidants

1.2.2.1 Catalase (CAT)

Catalase is one of the enzymes responsible for rapid detoxification of hydrogen peroxide to water and molecular oxygen. Catalases can be subdivided into three groups, based on differences in the sequence. Two of these groups are heme-containing catalases and the third possesses a dimanganese active site.

Heme-containing catalases are homotetrameric proteins. The hemes carrying iron atoms are buried deep in the protein and are only accessible to small molecules (such as hydrogen peroxide) via a narrow channel. The mode of action of these enzymes comprises two steps. The first step involves oxidation of ferriheme to an Fe(IV) porphyrin cation by one molecule of H_2O_2 (reaction 11), which is followed by reduction of this species back by another molecule of H_2O_2 and oxygen evolution (reaction 12) (*17*). Dimanganese catalases are homohexamers and work in a similar way as their heme-containing counterparts (reactions 13, 14). They are present in several bacterial species (*18*).

11. $\text{Fe(III) Por} + H_2O_2 + 2H+ \rightarrow \text{Fe(IV) Por}^+ + 2H_2O$
12. $\text{Fe(IV) Por}^+ + H_2O_2 \rightarrow \text{Fe(III) Por} + 2H^+ + O_2$

$\text{summary rxn} : 2H_2O_2 \rightarrow 2H_2O + O_2$

13. $2\ \text{Mn(III)} + H_2O_2 \rightarrow 2\ \text{Mn(II)} + 2H^+ + O_2$
14. $2\ \text{Mn(II)} + H_2O_2 + 2H^+ \rightarrow 2\ \text{Mn(III)} + 2H_2O$

$\text{summary rxn: } 2H_2O_2 \rightarrow 2H_2O + O_2$

1.2.2.2 Superoxide dismutase (SOD)

Superoxide dismutases are a family of metalloproteins that dismutate superoxide anion into water and hydrogen peroxide with the help of redox-active metal ion, such as copper, iron, manganese or nickel. The metal serves as an electron shuttle between two superoxide anions (*17*).

CuZnSOD is a homodimeric enzyme with two metal ions buried at the bottom of the funnel shaped active site of each subunit (*19*). This structure restricts the substrate only for negatively charged and small molecules like $O_2^{\bullet -}$ and its protonated form OH_2^-. Copper (II) acts as a catalytic centre, while zinc (II) plays rather a structural role. The copper (II) ion is

first reduced by superoxide molecule (reaction 15), and then reoxidized upon formation of OH_2^- from proton and superoxide (reaction 16). OH_2^- is further protonized to hydrogen peroxide after the release from the metal of the active site (reaction 17). CuZnSODs are present in cytosol, organelles and also in the extracellular space of eukaryotes (*17*).

15. $\text{E- Cu(II)} + O_2^{\bullet -} \rightarrow \text{E- Cu(I)} + O_2$
16. $\text{E- Cu(I)} + O_2^{\bullet -} + H+ \rightarrow \text{E- Cu(II)} + HO_2^-$
17. $HO_2^- + H^+ \rightarrow 2H_2O_2$

summary rxn: $O_2^{\bullet -} + O_2^{\bullet -} + 2H^+ \rightarrow H_2O_2 + O_2$

MnSODs and FeSODs are found mainly in prokaryotes and in specialized organelles (mitochondria or plastids), which is in accordance with the theory about endosymbiotic origin of these organelles. Mechanism of catalysis is also based on reduction and reoxidation of metal-ion centre (*17*).

Rather later discovered NiSOD is a type of SOD present in some prokaryotes (*20*). As nickel commonly exists in only one oxidation state in aqueous environment, it was suggested NiSODs may follow different reaction mechanism than other SODs (*21*).

1.2.2.3 Glutathione peroxidase (GPx)

Glutathione peroxidase is a glutathione-dependent protein responsible for reduction of various hydroperoxides, including hydrogen peroxide, small organic hydroperoxides or lipid hydroperoxides. Majority of GPx are tetrameric selenoenzymes, carrying a selenocysteine (Sec) residue at the active site (*22*). A unique amino acid, selenocysteine, is encoded by the TGA codon and a stem-loop selenocysteine insertion sequence (SECIS element) present in the 3‘-untranslated region (*23*). Selenium-containing GPx were described in mammals, some other vertebrates (*24*) and few invertebrate species (*25*).

On the other hand, homologues of GPx with cysteine residue instead of Sec also exist, being present especially among invertebrates. These Cys-GPxs do not always use GSH as a substrate, but may also prefer proteins with Cys-X-X-Cys motif (thioredoxin, tryparedoxin) as electron donors. Additionally, they follow catalytic mechanism similar to 2-cys peroxiredoxins, using two cysteine redox centers (*26, 27*). Despite the diversity of substrates, the structure of active site remains conserved in GPx. There is a specific catalytic tetrad

consisting of peroxidatic selenocysteine (cysteine), glutamine, tryptophan, and asparagine. Asn together with the Gln contribute to dissociation of selenol- (thiol-) group (*28*).

In general, the reaction catalyzed by GPx uses two molecules of reduced glutathione (GSH) to reduce one molecule of hydroperoxide (reaction 18). The mechanism of this catalysis is not fully understood, but it certainly includes oxidation and reduction half-reaction, the latter occurring in two steps (Figure 1)(*29*).

18. $ROOH + 2\,GSH \rightarrow GSSG + ROH + H_2O$

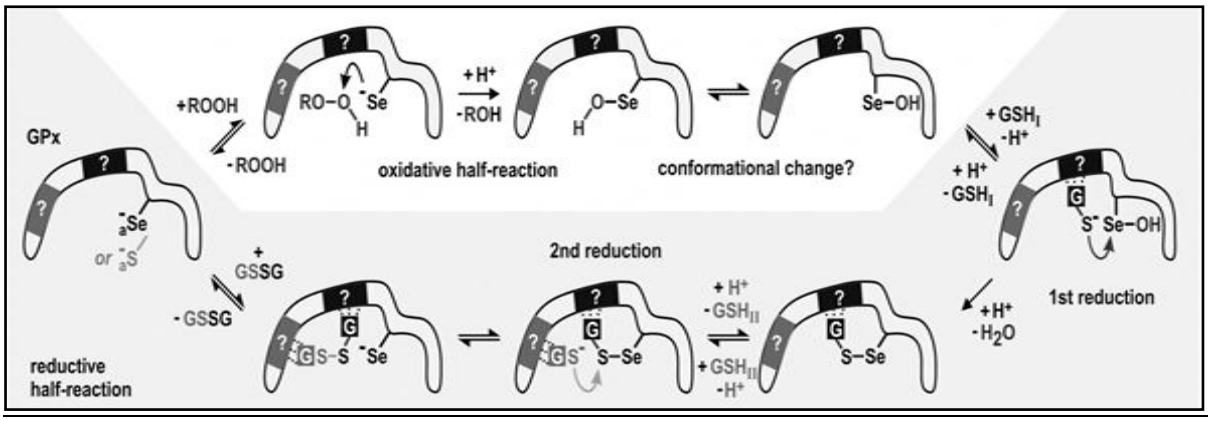

Figure 1: Model of glutathione-dependent GPx catalysis. The active site either contains a deprotonated selenocysteine or cysteine residue. The reaction proceeds in two half-reaction steps. At first, the selenocysteine (cysteine) residue is oxidized by hydroperoxide to selenenic (sulfinic) acid. Then, the first molecule of GSH binds to the protein and reduces the acid intermediate. Reaction of the second GSH directly follows, yielding GSSG and recycling the protein redox centre. Adapted from (*29*).

1.2.2.4 Peroxiredoxin (Prx, Prdx)

Peroxiredoxins are a family of ubiquitous proteins that are highly conserved across the phylla. They are responsible for detoxification of hydrogen peroxide (*30*), various organic hydroperoxides (*31*) or peroxinitrites (*32*, *33*) (simplified in reaction 19). Their functions partly overlap with catalases or glutathione peroxidases (*34*). Former name of peroxiredoxins - thioredoxin peroxidases - reflects the fact that thioredoxin was found to be an electron donor for their reactions. Later, the name peroxiredoxins (Prx, Prdx) was suggested for the reason that not all enzymes from the family seem to use thioredoxin as an electron donor (*35*).

19. $R'\text{-}SH + ROOH \rightarrow R'\text{-}S\text{-}S\text{-}R' + H_2O + ROH$ (R = alkyl, -H, R'= various reductants)

Classification

The activity of peroxiredoxins is based on redox-active cysteine residues, which participate in reduction of peroxides. From the mechanistic point of view, peroxiredoxins are classified

into three subgroups - 2-Cys peroxiredoxins, atypical 2-Cys peroxiredoxins and 1-Cys peroxiredoxins - depending on the number and the position of cysteine residues participating in the catalysis (Figure 2). Two-Cys Prxs contain two conserved cysteine residues, a peroxidatic cysteine and a resolving cysteine, whereas one-Cys Prxs possess only the peroxidatic residue (*34*).

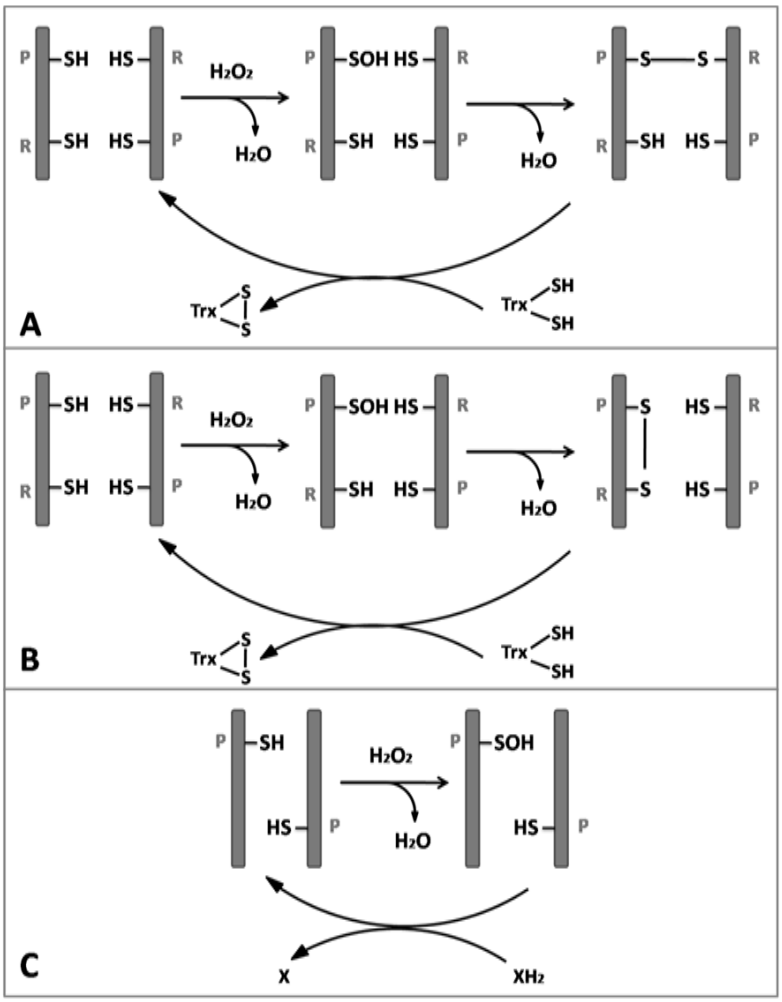

Figure 2: Mechanistic classification of peroxiredoxins. A=typical 2- Cys Prx, B=atypical 2-Cys Prx, C=1-Cys Prx. Typical 2-Cys Prx forms an intersubunit disulfide bond with resolving cysteine, while atypical 2-Cys Prx forms an intrasubunit disulfide. Both use thioredoxin as a preferential electron donor. One-Cys Prx retains only peroxidatic cysteine and its recycling occurs via unspecified electron donor. P=peroxidatic, R=resolving, Trx=thioredoxin, X=unspecified donor. Adapted from (*36*).

There are also attempts to establish new classification of enzymes from peroxiredoxin family. A PREX database divides the peroxiredoxins into six subfamilies according to the structure and sequence of the active site (Table 1)(*37*). This classification does not exactly overlap with earlier mechanistic classification, as some of the six subclasses contain representatives of both 1-Cys and 2-Cys group (*38*). Recently, the new classification has been employed also in PeroxiBase, a database specialized on peroxidases.

Table 1: Classification of Prx into six subfamilies according to structural analysis and active site profiling method. AhpE subfamily contains only few members and the presence of resolving cysteine was not detected in all of them. Ahp= alkyl hydroperoxide reductase, BCP= bacterioferritin comigratory protein, TPx= thiol peroxidase, Prx= peroxiredoxin. C_R= resolving cysteine. Adapted from (*37*) and (*39*).

subfamily	example	C_R	oligomeric form	mechanistically
Prx1/AhpC	*H. sapiens* Prx 1-4 *S. typhimurium* AhpC	yes	dimer decamer	typical 2-Cys Prx
Prx6	*H. sapiens* Prx6	no	dimer may form decamer	mainly 1-Cys Prx
Prx5	*H. sapiens* Prx5	yes	dimer	atypical 2-Cys Prx
BCP/PrxQ	*E.coli* BCP, plant PrxQ	yes	typically monomer may form dimer	atypical 2-Cys Prx
TPx	*E. coli* Tpx	yes	dimer	atypical 2-Cys Prx
AhpE	*M. tuberculosis* AhpE	?	dimer (?)	?

Catalytic cycle

The first step of Prx catalysis, peroxidation, is common to all Prx groups. Peroxidatic cysteine, positioned at the N-terminal end of the protein, attacks the peroxide substrate and is oxidized to cysteine sulfenic acid. The second step, resolving, is achieved by the formation of a disulfide bond with the resolving cysteine of Prx itself or another protein. In typical 2-Cys peroxiredoxins, disulfide bridge is formed between two neighboring subunits of Prx dimer. Atypical 2-Cys Prxs, on the other hand, form an intramolecular bridge. In one-Cys peroxiredoxins, resolving follows different pathway involving other thiol-containing molecule. The third step, the recycling of peroxidatic cysteine residues, occurs via a specific electron donor (*38*). Preferential electron donor for this step in most Prx is thioredoxin. Both typical and atypical 2-Cys Prx seem to use this reductant, although some specialized proteins such as tryparedoxin or AhpF and AhpD may also act in similar way (*40*). For one cysteine peroxiredoxins, the identity of physiological redox partner is still unclear (*38, 41*). The catalytic cycle involves structural change from fully folded to locally unfolded state and back (*38*).

Active site

The structure of the active site of all peroxiredoxins is highly conserved. Beside the active-site peroxidatic cysteine, there is an arginine residue in its close proximity that helps the stabilization of thiolate ion. Two more residues contribute to functionality of the active site – proline, closing off one side of the active site pocket, and threonine, hydrogen bonded to peroxidatic cysteine (Figure 3). These create a motif **P**-X-X-X-**T**-X-X-**C_P** (*34*, *42*)**.**

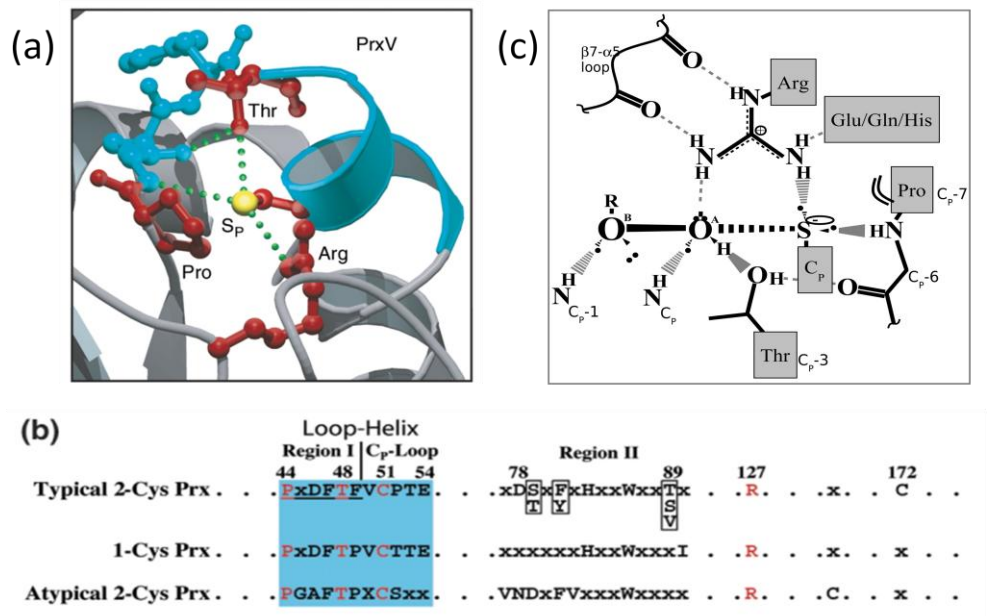

Figure 3: (a) Conserved residues of Prx active site (Pro, Arg, Thr) and hydrogen bonding network. The active site is located in helix-loop region. (b) The alignment of sequences for the three Prx classes representing the consensus sequence with conserved active site residues. Numbering of residues is according to PrxV. (c) Interactions at Prx active site after binding of peroxide substrate. Adapted from (*34*) and (*43*).

- **<u>Typical two-Cys peroxiredoxins</u>**

Typical 2-Cys peroxiredoxins are the most numerous group of Prx. They usually use thioredoxin as a redox partner for peroxide reduction, but not glutathione or glutaredoxin (*36*). Beside the peroxidase activity, they also play a role in cellular signaling or as molecular chaperones.

During the catalysis, 2-Cys Prxs shift the structure between a dimer and a decamer consisted of five dimers (*44*). The oligomeric state depends particularly on redox state of the protein and phosphorylation events (*38*).

Prx can regulate hydrogen peroxide intracellular messenger function. Two main ways of this regulation were suggested, based on the inactivation of Prx enzyme. First of them is the

temporary overoxidation of catalytic cysteine residue to sulfinic acid. This process requires all catalytic components (H_2O_2, Trx/TrxR, NADPH) (*45*) and is reversible by the action of sulfiredoxin (*46*). Another type of regulation of Prx activity occurs via Prx phosphorylation by cyclin-dependent kinases (*47*).

Prx can also exhibit molecular chaperone activity, preventing protein aggregation (*48*). While peroxidase function predominates in low molecular weight Prx complexes, molecular chaperone activity has been attributed to decameric or higher oligomeric structures (*40, 49*). The functional switch from peroxidase to molecular chaperone upon structural change was shown to be triggered by hyperoxidation of peroxidatic cysteine to sulfinic acid (*40, 50*). In human PrxII, YF motif in C-terminal domain was also found to contribute to structural change (*50*).

- **Atypical 2-Cys Peroxiredoxins**

The class of atypical 2-Cys Prx consists of Prx that have two cysteine residues participating in catalytic cycle. Comparing to typical 2-Cys Prx, only the peroxidatic Cys is conserved. Resolving Cys position is variable and does not show sequence similarity with typical 2-Cys Prx. The two cysteine residues form an intramolecular disulfide bond during the catalysis, which is disrupted by the action of thioredoxin (*36*). Concerning the substrate, members of this family prefer alkyl hydroperoxides over H_2O_2 (*51, 52*).

Mammalian Prx 5 is the most studied representative of this group. Among others, bacterial BCP (*53*) and TPx (*54, 55*) as well as plant PrxQ (*56*) also belong to this family.

- **One-Cys peroxiredoxins**

Although 1-Cys Prxs show similarities to other Prx groups, they have some unique properties that are restricted only to them. Firstly, 1-Cys Prxs contain only the peroxidatic cysteine residue. In most cases, catalytic cycle does not involve thioredoxin as the electron donor. Moreover, some members of this group exhibit also Ca^{2+}-independent phospholipase activity in addition to peroxidase activity (*35, 41*).

Substrates for 1-Cys Prxs are hydrogen peroxide, short chain hydroperoxides (Manevich 2005), as well as phospholipid hydroperoxides which are not typical substrates for other Prxs (*57*). The peroxidase motif around catalytic active site, PVCTTE, is with small variations

conserved in all 1-Cys members (*58*). The pH maximum for peroxidase activity is between 7 and 8, which consistent with its cytosolic localization (*59*).

There is a controversy accompanying the search for physiological reductant of 1-Cys Prx, and many candidates were already tested. Thioredoxin, the primary source of electrons for 2-Cys Prx, was found ineffective with several Prx (*57*, *60*), but worked for others (*61*, *62*). Glutathione-dependent activity was investigated with similar results. GSH worked as a reductant in certain studies (*63*, *64*), but failed in some others (*30*, *65*). On the other hand, Prxs from some organisms accepted both of the above mentioned electron donors (*62*). Manevich and colleagues (*66*) concluded that Prx heterodimerized with π glutathione-S-transferase undergoes glutathione-dependent reaction in comparison to sole Prx. Yet another substances were tested as potential redox partners of 1-Cys Prx including ascorbate (*67*), glutaredoxin (*68*) or cyclophylin (*69*).

Some 1-Cys Prxs were found to have dual activity - as peroxidases and Ca^{2+}-independent phospholipases A_2 ($iPLA_2$). The latter are responsible for hydrolysis of sn-2 ester bond of phospholipids (*70*). Lipase motif (GXSXG) with serine as a catalytic centre was found in several species (*58*). The phospholipase activity was confirmed in some mammals, including human (*71*), rat (*72*) or cow (*73*). The $iPLA_2$ pH optimum is in acidic (around pH 4) range, indicating the main activity in lysosomes (*58*).

1.2.2.5 Thioredoxin and glutathione/glutaredoxin systems

Thioredoxin system consists of NADPH, thioredoxin (Trx) and thioredoxin reductase (TrxR). Trx serve as a thiol reductant for disulfide substrates and for the regeneration of enzymes such as peroxiredoxins or methionine sulfoxide reductases. It is converted back to the reduced form via the action of NADPH-dependent TrxR (*74*).

Similarly, glutathione system is based on glutathione (GSH), which serves as an electron donor for glutathione peroxidases and small antioxidant molecules. Oxidized glutathione (GSSG) is regenerated via NADPH-dependent glutathione reductase (GR). Glutaredoxin (Grx) system is coupled to glutathione system and uses GSH for glutathionylation of thiol-containing proteins. This protein modification is reversible and can either activate or inactivate the target protein. Deglutathionylation occurs via Grx reductase (GrxR), which also uses NADPH as a reducing equivalent (*75*).

Both thioredoxin and glutathione systems may be present in the cells and function in parallel, together regulating the cell redox homeostasis (Figure 4). Some of the components of the individual system may even cross-react with the other system (*75*).

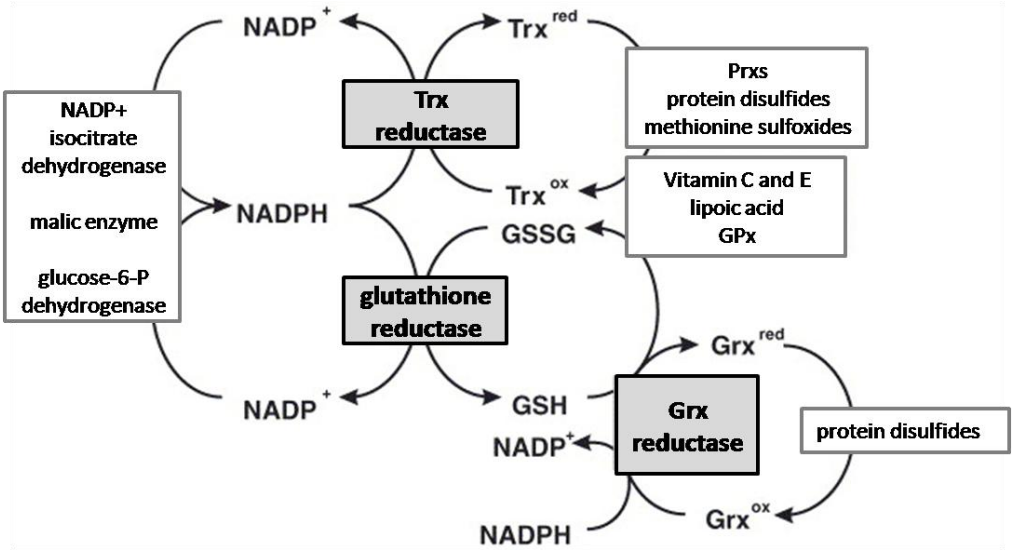

Figure 4: Schematic representation of thioredoxin, glutathione and glutaredoxin system and their cooperation. NADPH, the major cell reductant, is a source of electrons for the redox cycles. NADPH/NAD$^+$ = reduced/oxidized nicotine adenine dinucleotide phosphate; GSH/GSSG = reduced/oxidized glutathione, Trx = thioredoxin; Grx = glutaredoxin; Prxs = peroxiredoxins; GPx = glutathione peroxidase; Adapted from (*76*).

1.3 Ticks

Ticks are blood-feeding ectoparasites of vertebrates. They belong to the class Arachnida, subclass Acari, order Ixodida. They are divided into three families, Ixodidae, Argasidae and Nuttallidae, a small family comprising only one species. Ixodidae are also called hard ticks, because they have chitinized dorsal scutum, whereas Argasidae, soft ticks, have only leathery scutum (*77*).

Ticks transmit the variety of pathogens, including bacteria (*Rickettsia*, *Borrelia*, *Ehrlichia*, *Anaplasma*, *Francisella*), viruses (tick-borne encephalitis virus, Crimean-Congo hemorrhagic fever virus) and protozoans (*Babesia*). These pathogens cause serious diseases both in animals and human (*78*).

Ixodes ricinus

Ixodes ricinus, also called castor bean tick or European sheep tick, is ther main European representative of the hard tick family. It can be found in relatively humid areas of woodlands and forests. It has a three host life cycle, with each developmental stage feeding on a single host (Figure 5). Larvae prefer feeding on small vertebrates (e.g. rodents, insectivores, birds

or reptiles), nymphs feed typically on middle-sized animals (e.g. rabbits) and adults feed mainly on larger mammals (sheep, cattle and deer). Human is a potential host for all stages (*79*). Most common pathogens transmitted by *I. ricinus* are tick-borne encephalitis virus (TBEV), responsible for tick-borne encephalitis infection, and spirochetes of *Borrelia burgdorferi* sensu lato complex, causative agents of Lyme disease (*80*).

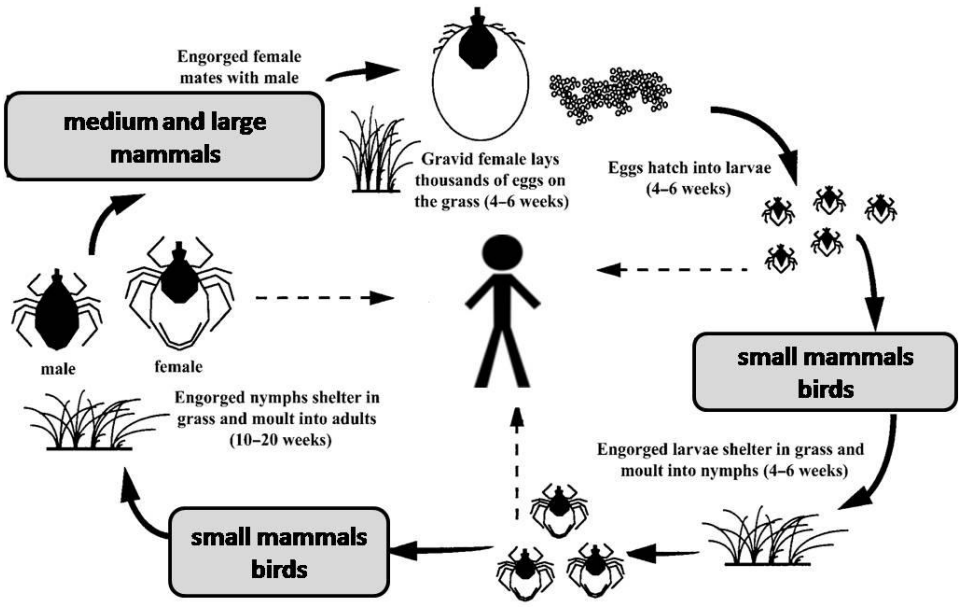

Figure 5: The life-cycle of *Ixodes ricinus*. Each stage of the tick seeks for a host, attaches, and then feeds until repletion. Afterwards, the tick drops off to molt to the next feeding stage. Only adult female feeds on a host, where the mating occurs at the same time. Fed adult female lays several thousands of eggs and then die. Adapted from (*81*).

1.4 Oxidative stress and antioxidant defense in ticks

The hematophagous lifestyle brings some problems ticks have to deal with. These include production of ROS and consequently a potential risk of oxidative stress. In this respect, ticks may be endangered by ROS produced at two instances: 1) during blood digestion in the midgut and 2) at the tick-host interface by the host immune response to tick bite.

Hemocytes, the immune cells from tick hemolymph, were also shown to generate ROS in response to PMA activation or incubation with bacteria. This suggests their action is similar to vertebrate phagocytic cells, i.e. they are involved in tick defense against pathogens (*82*).

Both the internal and external ROS insults may be prevented by the action of antioxidant enzymes (*83*). In the following sections, the attention will be paid to the ROS produced in response to blood-feeding and the corresponding antioxidant defense.

1.4.1 Blood digestion-induced oxidative stress

Ticks, as hematophagous animals, ingest large amount of blood. They are able to increase their body weight as much as several hundred times during the feeding process (*84*). Hemoglobin serves as a major source of nutrient for them, but its degradation represents a possible threat due to high concentration of produced heme molecules (*85*). Heme is a prosthetic group of hemoglobin and consists of porphyrin ring enclosing an iron atom (*86*).

Heme toxicity

Heme is a potentially toxic substance, because it is a lipophilic molecule with ability to interact with membranes and cause their leakage (*87*). In addition, it is able to generate ROS (*88*). Although it is not the only source of ROS in the organism, it contributes to the amplification of negative ROS effects (*85*). The major pathway of heme-induced ROS production is the decomposition of organic hydroperoxides, leading to the formation of alkoxyl and peroxyl radicals (*89*). Fenton oxidation was also proposed as a source of hydroxyl radicals (*90*), even though some doubts have risen about heme being a Fenton reagent (*91*). All the above mentioned radicals contribute to lipid peroxidation (*85*).

Adaptations of ticks to heme toxicity

Ticks, similarly to other blood-feeders, developed multiple adaptations to heme toxicity (Figure 6). Digestion of vertebrate blood in ticks is an intracellular process, taking place in digestive cells of midgut. Blood components are endocytosed and huge amounts of heme are released from hemoglobin. Most of the free heme molecules are aggregated to larger structures in specialized organelles called hemosomes (*92*). In this way, heme is less accessible to peroxidation events. The transportation of heme between digestive vesicles and hemosomes is probably mediated by heme-binding proteins (*93*).

Heme-binding proteins, such as HeLp described in *R. microplus*, play also an important role in protection from heme-induced oxidative damage. They bind free heme molecules so they could not react with oxygen species, and carry them to tick tissues for incorporation into other proteins (*94*). Other heme-binding proteins were also found in *D. variabilis* (*95*) or *D. marginatus* (*96*).

For the purpose of maintaining heme homeostasis, it is further degraded into biliverdin, carbon monoxide and Fe^{2+} by the action of heme oxygenase (*97*). Potentially dangerous

ferrous ions produced by the degradation then have to be chelated by ferritin to avoid undesirable Fenton reaction (*91*).

At last, low molecular antioxidants and antioxidant enzymes represent indispensable part of heme detoxification mechanism. These will be described in next section.

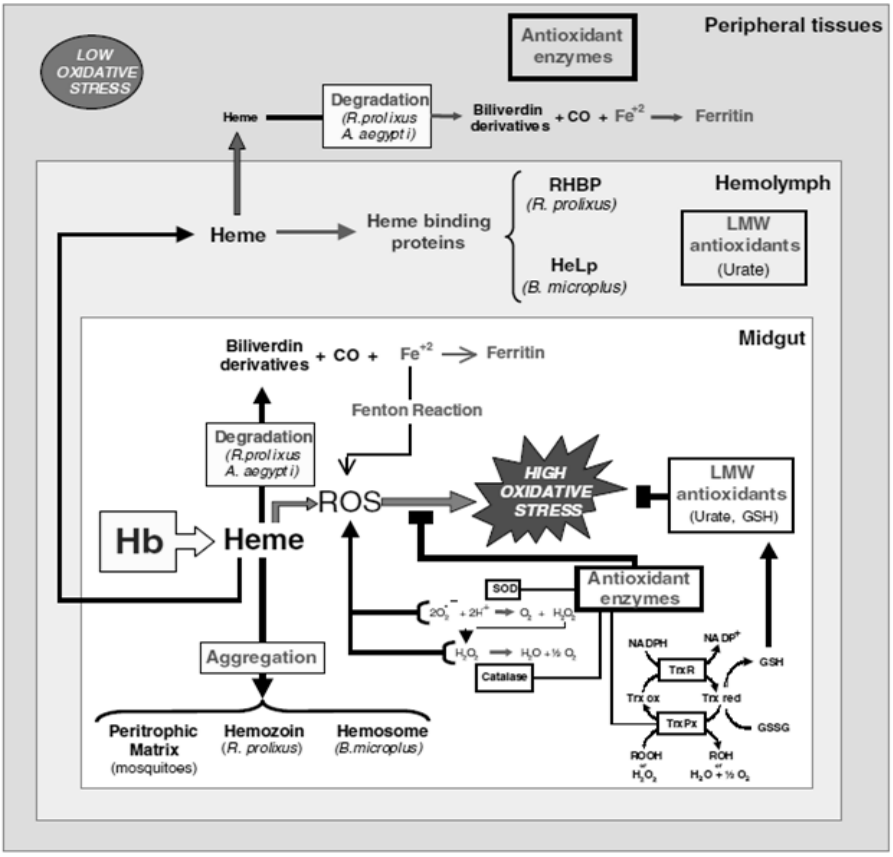

Figure 6: Major adaptations of blood-feeding animals to heme toxicity: formation of heme aggregates, heme degradation, antioxidant enzymes, low molecular weight radical scavengers and heme-binding proteins. Hb-hemoglobin; ROS- reactive oxygen species; SOD-superoxide dismutase; TrxR-thioredoxin reductase; TrxPx-thioredoxin peroxidase; Trx red-reduced thioredoxin; Trx ox-oxidized thioredoxin; GSH-reduced glutathione; GSSG-oxidized glutathione. Adapted from (*85*).

Antioxidants involved in heme detoxification

The knowledge about the role of antioxidants in ticks' blood digestion is very limited. The pioneering work is that of Citelli and colleagues (*98*). This study was focused on the role of catalase in the control of redox balance in the tick *Rhipicephalus microplus.* After the injection of catalase inhibitor into the ticks, they observed the increased peroxide levels in the gut, which lead to lower egg-laying rates and diminished the ticks' lifespan. The digestive gut cells of these ticks displayed altered morphology, with heme spread all over the cytosol instead of being aggregated in hemosomes. Additionally, ticks fed on CAT inhibitor-treated cattle suffered from similar problems as injected ticks.

Despite the fact that the action of antioxidants is very little explored in ticks, we may deduce its importance from the studies of antioxidants in other blood-feeding arthropods. Increased expression of stress enzymes, particularly those from thioredoxin system (TrxR/Trx), were observed in mosquitoes *Anopheles gambiae* (*99*) and *Aedes aegypti* (*100*) after the blood meal. In a triatomine insect *Rhodnius prolixus*, high levels of urate in the hemolymph as well as significant midgut activities of SOD and catalase were found. Inhibition of glutathione and catalase synthesis in this species resulted in the increased production of H_2O_2 in midgut (*101*). Silencing of catalase gene in *Anopheles gambiae* or *Lutzomyia longipalpis* influenced their mortality and reproduction capability after blood ingestion (*102*, *103*).

1.4.2 Oxidative stress within tick-host interface

Characterization of tick-host interface

After initiation of blood-meal, ticks experience multiple host defense mechanisms including blood coagulation, platelet aggregation, vasoconstriction (Figure 7) and both innate and adaptive immune responses (Figure 8) (*104*, *105*). For that reason, their salivary glands secrete a wide range of pharmacologically active molecules with anti-haemostatic, anti-inflammatory and immunomodulatory functions (*99*). This helps them to counterbalance the host response and accomplish the feeding process. Many of these salivary components are expressed in response to feeding and their levels may vary with feeding time (*106*).

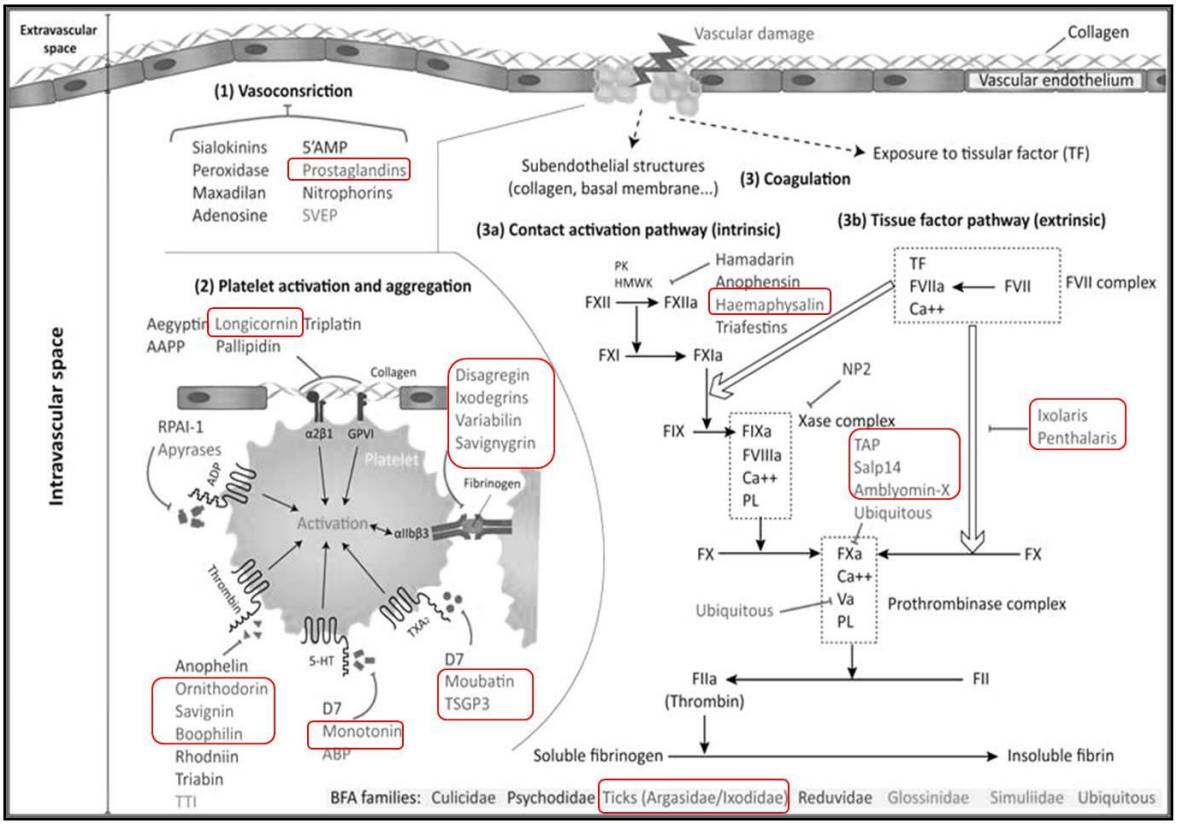

Figure 7: Schematic modes of action of arthropod salivary components involved in modulating host haemostatic defense. These proteins act mainly as vasodilators, inhibitors of platelet aggregation and anticoagulants. Tick components are highlighted (red boxes). Adapted from (*105*).

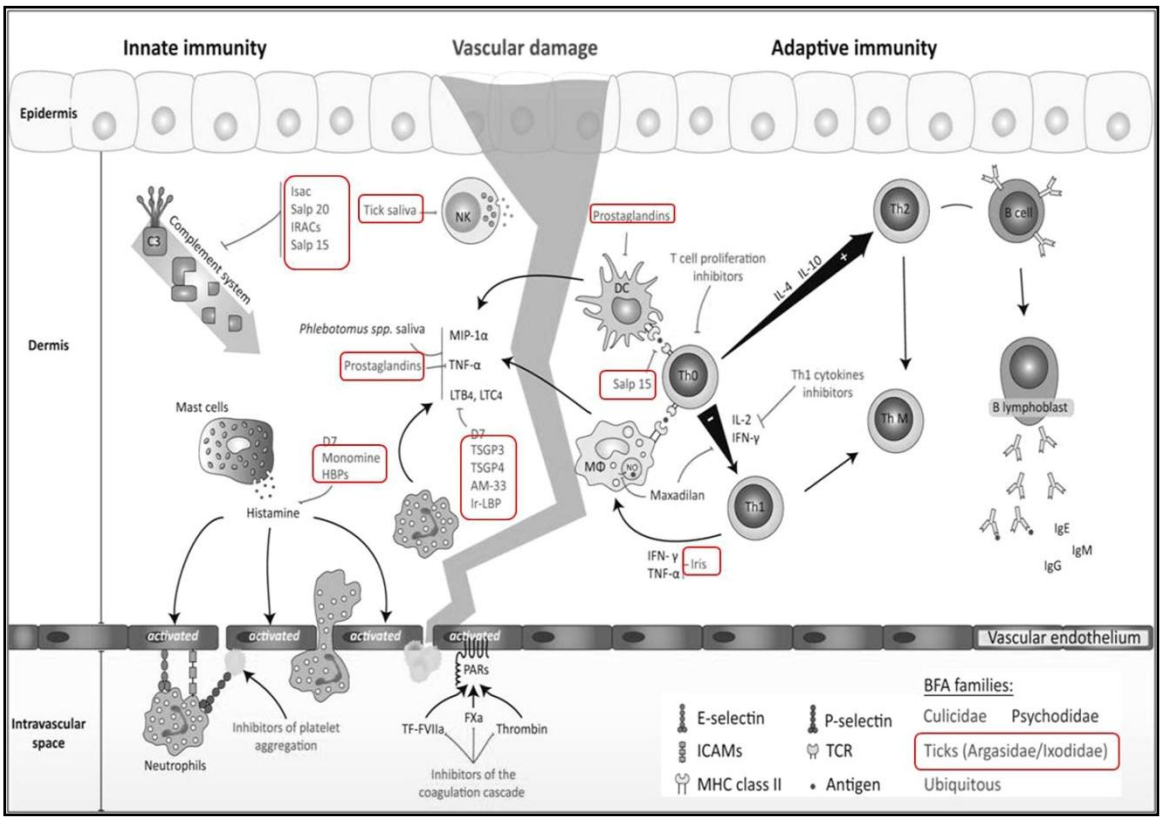

Figure 8: Schematic modes of action of arthropod salivary components involved in modulating host innate and adaptive immune response. They exhibit mainly anti-inflammatory, anti-complement or T-cell modulatory activities. Tick components are highlighted (red boxes). Adapted from (*105*).

ROS and antioxidants

To start feeding, tick has to pierce host skin with its hypostom. In response to the skin injury, innate immune system reacts by migration of phagocytic cells such as neutrophils and macrophages to the wound site. These cells get activated and produce variety of pro-inflammatory molecules as well as reactive oxygen species as a defense against invading bacteria (*107*). Potential threat of ROS-mediated tissue damage must be prevented by the action of antioxidants.

Indeed, antioxidant enzymes were found in tick saliva. Peroxidases with homology to 1-cys peroxiredoxins (or PrxVI) were detected in hard ticks *Heamaphysalis longicornis* (*83*) and *Ixodes scapularis* (*108*).

Peroxiredoxin from *H. longicornis* (HlPrx) was identified by using degenerate primers designed on the conserved regions of Prx genes. The secretion in tick saliva was confirmed by immunoblot of infested rabbit sera with recombinant HlPrx. Localization in the salivary glands was further explored via immunohistochemical assay. A recombinanly prepared HlPRx showed *in vitro* antioxidant activity in metal-catalyzed oxidation system (*83*).

On the other hand, peroxidase named Salp25D from *I.scapularis* was identified using immunoscreening of a cDNA library. Sera of tick-infested rabbits reacted with salivary gland extract, confirming its presence in tick saliva. Recombinant protein also showed *in vitro* antioxidant activity in metal-catalyzed oxidation system and catalyzed glutathione-dependent hydrogen peroxide reduction (*108*). In addition, the protein was able to quench oxygen radicals produced by activated neutrophils *in vitro* (*109*).

In spite of being found in tick saliva, both of these peroxidases lack N-terminal leader sequence characteristic for secreted protein. It was suggested that they may be incorporated into the saliva by cell degradation or leakiness (*108*) or follow an alternative secretory pathway (*83*). A non-classical secretion was already observed in some antioxidant proteins (*110*).

Tick-host-pathogen interface

The set of biologically active salivary molecules is highly beneficial, not to say crucial, for pathogens using the ticks as the vectors. Thereby, they are able to evade the host immune response and are successfully transmitted to a vertebrate host. This event is termed “saliva activated transmission” or “SAT” (*111*) and is supported by several direct and indirect

evidences. A direct evidence of SAT is based on the studies of the impact of salivary gland extracts on pathogen infectivity (*112–115*). Indirect confirmation of the phenomenon is provided by the observation of non-systemic transmission of pathogens by tick co-feeding on the same host (*116–118*).

Multiple studies are dedicated to the effects of tick saliva on *B. burgdorferi* species, especially on the transmission and infectivity of pathogens in the presence of SGE (*114*, *115*, *119–122*) and on SGE-pathogen interaction *in vitro* (*123*, *124*). Moreover, few specific salivary proteins involved in SAT events have been already described. *I. scapularis* Salp15 was shown to bind OspC of *B. burgdorferi*, thus facilitating spirochete transmission (*125*). Anti-complement proteins of the same tick, Isac and Salp20, can inhibit complement-mediated killing of borrelia (*126*, *127*).

With respect to the tick antioxidant proteins, the role of *I. scapularis* peroxiredoxin Salp25D in acquisition and transmission of *B. burgdorferi* was studied in more detail. After the silencing of the salivary Salp25D, acquisition of spirochetes by ticks fed on infected host was significantly decreased. The effect of knock-down on transmission from infected tick to uninfected host was not confirmed, but further investigation in this field may be required. Secondly, the immunization of infected mice with recombinant Salp25D resulted also in the impaired acquisition of spirochetes by ticks (*109*).

Identification of tick salivary components mediating SAT is a challenge that may provide new ways of controlling ticks and tick-borne pathogens (*111*).

1.5 Anti-tick vaccines

Upon tick infestation, the host can develop antibodies against the encountered tick antigens and thus can be protected from subsequent tick bites. This phenomenon is known as acquired immunity to ticks and is a key idea for the development of anti-tick vaccines (*108*, *128*). The immunological resistance to ticks is characterized by reduced weight of tick, prolonged feeding periods, reduced number of ova, impaired molting and eventually tick death (*129*).

Apart from tick control, such vaccines may be also useful for blocking of pathogen transmission, as tick-immune hosts show disruption of the transmission process (*129*, *130*). Prevention of tick-borne diseases by means of such vaccines would be an alternative to problematic design of vaccines based on pathogen-derived antigens (*131*).

Using of tick antigens for the tick control is an appealing concept, which has several advantages. In comparison to currently used acaricide applications, antigen-based vaccines would not represent a risk for the environment, would be more specific and potentially even cost-effective. Additionally, the problem with acaricide resistance would be avoided (*132*).

Several tick proteins have been proposed as vaccine candidates and tested in immunization studies. These include, among others, gut proteins Bm86 and Bm95 from *R. microplus* (*133*), salivary cement protein 64TRP from *R. appendiculatus* (*134*), subolesin from *I. scapularis* (*135*), serpin from hemolymph of *H. longicornis* (*136*) or ferritin 2 from *I. ricinus* (*137*). Tick salivary antigens were also found to be suitable candidates due to their presence at tick-host-pathogen interface. *I. scapularis* salivary proteins like Salp15 (*138*), sialostatin L2 (*139*), Isac (*140*) or even a mixture of salivary antigens (*140*) were tested as vaccines for blockage of tick feeding and transmission of *B. burgdorferi*.

Antioxidant Salp25D from *I. scapularis* was also suggested as one of the candidate proteins. Immunization of *Borrelia*-infected mice prevented ticks from pathogen acquisition (*109*). Further, it was employed in immunization of murine host with mixture of antigens (Salp15, Salp25A, Salp25D and Isac) cloned into an adenoviral vector. No effects on feeding were observed, but there was a decrease in spirochete load in the host's heart in comparison to control (*140*).

To find a way for the development of an efficient vaccine, few strategies were proposed. The use of highly conserved antigens or antigens with immune cross-reactivity could be applicable to wide range of tick species. A combination of tick antigens might enhance the protective effect of the vaccine. Recently, methods of RNA interference are used for the characterization of the tick protective antigens, which may enable the design of new vaccines (*132*).

1.6 Salp25D from *Ixodes ricinus*

A homologue of peroxiredoxin was found in *I. ricinus* whole body subtracted cDNA library that was enriched with differentialy expressed tick genes induced by blood feeding or borrelial infection. The gene has 666 bp and encodes protein with 221 amino acids and molecular weight of 24,5 kDa. It was determined that it does not contain any introns and lacks the N-terminal signal peptide. The gene for Salp25D was isolated and cloned into an expression vector. Preliminary pilot expression and purification experiments were performed (*141*).

The stage- and tissue-specific expression of Salp25D was performed using semi-quantitative RT-PCR. Gene expression was observed in all developmental stages of *I. ricinus* and all organs, with preferential expression in salivary glands, midgut and ovaries. The expression seemed to be slightly increased after blood-feeding (*141*).

2 GOALS OF THE WORK

- Preparation of recombinant Salp25D (optimization of expression and purification procedures).
- Analysis of rSalp25D ability to protect supercoiled DNA from hydroxyl radical-mediated damage.
- Analysis of rSalp25D ability to protect *Borrelia burgdorferi* from hydroxyl radical-mediated killing.
- Testing of glutathione as a possible electron donor for a reaction catalyzed by rSalp25D.
- Silencing of Salp25D in *I.ricinus* and confirmation of the knockdown by quantitative RT-PCR.

3 MATERIALS

3.1 Chemicals, buffers, media

Table 2: Material for the recombinant protein production

Expression in bacterial system	
Expression vector (Invitrogen)	Champion pET100/D-TOPO
Bacterial system (Invitrogen)	BL21 Star™ (DE3) One Shot® *E. coli*
Luria-Bertani Broth, Miller/ LB (Amresco)	1% tryptone, 0.5% yeast extract, 1% NaCl, pH 7.0
Ampicillin (Sigma-Aldrich)	50 mg/ml stock solution, 50 μg/ml working solution
S.O.C. medium (Invitrogen)	2% tryptone, 0,5% yeast extract, 10 mM NaCl, 2.5 mM KCl, 10 mM $MgCl_2$, 10 mM $MgSO_4$, 20 mM glucose
Isopropyl β-D-1-thiogalactopyranoside/ IPTG (Sigma-Aldrich)	1M stock solution, 1mM working solution
Tris-EDTA buffer/ TE	10 mM Tris-HCl (pH 8.0), 1 mM EDTA (pH 8.0)
Recombinant protein purification	
Lysis buffer	50 mM NaH_2PO_4, 300 mM NaCl, 10 mM imidazole, pH 8.0
Washing buffer	same as lysis buffer, 20 mM imidazole
Washing buffer 2	same as lysis buffer, 50 mM imidazole
Elution buffer	same as lysis buffer, 250 mM imidazole
Lysozyme (Serva)	1 mg/1 g resuspended cells
Protease Inhibitor Cocktail for His- tagged proteins (Sigma-Aldrich)	AEBSF, Bestatin, E-64, Pepstatin A, Phosphoramidon
Ni-NTA Agarose (Qiagen)	50% suspension in 30% ethanol
Dialysis	
10x phosphate buffered saline/ PBS	1.37 M NaCl, 27 mM KCl, 54 mM Na_2HPO_4, 5,66 mM KH_2PO_4
SDS-PAGE	
4x DualColor protein Loading Buffer (MBI Fermentas)	0.25 M Tris-HCl (pH 8.5 at 25°C), 8% SDS, 1.6 mM EDTA, 0.024% Pyronin Y, 0.04% Bromophenol blue and 40% glycerol
20x Reducing Agent (MBI Fermentas)	2M DTT
40% Acryl/Bis (Amresco)	acrylamide: bisacrylamide 37.5:1
Tris-HCl (stacking gel)	0.5 M Tris-HCl, pH 6.8
Tris-HCl (resolving gel)	1.5 M Tris-HCl, pH 8.8
Sodium dodecylsulphate/ SDS (Sigma-Aldrich)	10% stock solution
N,N,N',N'- tetramethylenediamine /	

TEMED (Sigma-Aldrich)	
Ammonium persulphate/ APS (Sigma-Aldrich)	10% stock solution, freshly prepared
Tris-glycine running buffer 5x	25 mM Tris, 250 mM glycine, 0.1% SDS
Gel staining solution (MBI Fermentas)	PageBlue Protein Staining Solution
PageRuler Plus Prestained Protein Ladder (MBI Fermentas) Prestained Protein Marker Broad Range (NEB)	
Western blot	
Blotting buffer	25 mM Tris, 192 mM glycine, 4% methanol
TBS	10 mM Tris-HCl, pH 7.5, 150 mM NaCl
TBS-Tween	20 mM Tris-HCl, pH 7.5, 500 mM NaCl, 0.05% v/v Tween 20
10x Tris-saline	9% NaCl in 1M Tris-HCl, pH 8.0
Ni-NTA HRP Conjugate (Qiagen)	
HRP staining solution	3.3 mM 4-chloro-1-naphtol, 20% methanol, 80% 1x Tris-saline, 0.06 % H_2O_2

Table 3: Material for PCR and agarose gel electrophoresis

PCR	
2x PCR Master Mix (Promega)	50 units/ml Taq DNA polymerase, 400 μM dNTPs (each), 3 mM $MgCl_2$
agarose gel electrophoresis	
Agarose SERVA for DNA electrophoresis (Serva)	
1x Tris-acetate-EDTA buffer/ TAE	40 mM Tris, 20 mM acetic acid, 1 mM EDTA
6x Blue/Orange Loading Dye (Promega)	0.4% orange G, 0,03% bromophenol blue, 0.03% xylene cyanol FF, 15% Ficoll® 400, 10 mM Tris-HCl (pH 7.5), 50 mM EDTA (pH 8.0)
10 000x SYBR Gold nucleic acid gel stain (Invitrogen)	
25 bp DNA Ladder (Invitrogen)	
O'GeneRuler 1 kb DNA Ladder (MBI Fermentas)	
GeneRuler 100 bp Plus DNA Ladder (MBI Fermentas)	

Table 4: Material for functional experiments

DNA nicking assay	
Metal - catalyzed oxidation system	3 μM $FeCl_3.2H_2O$, 10 mM DTT, 0,1 mM EDTA
Supercoiled pBR322 plasmid (Inspiralis)	1mg/ml in TE
1 M HEPES Solution (Sigma-Aldrich)	
Borrelia viability assays	
Metal – catalyzed oxidation system	as above
1 M HEPES Solution (Sigma-Aldrich)	
Propidium iodide (Sigma-Aldrich)	500 μg/ml stock solution
GPx activity assay	
Potassium phosphate buffer, pH 7	61.5 % 1M K_2HPO_4, 38.5 % 1M KH_2PO_4
Glutathione, reduced/ GSH (Sigma-Aldrich)	
Glutathione Reductase from Baker's Yeast/ GR (Sigma-Aldrich)	100 U, suspension in 3.6 M $(NH4)_2SO_4$, pH 7.0
Glutathione Peroxidase from Bovine Erythrocytes (Sigma-Aldrich)	100 U, lyophilized powder
NADPH reduced form (Sigma-Aldrich)	
30% hydrogen peroxide /H_2O_2 (Lach-ner)	

Table 5: Material for RNA interference

RNA interference	
Plasmid digestion and ligation	
Restriction enzymes (MBI Fermentas)	FastDigest XhoI, FastDigest XbaI, FastDigest ApaI
10x FastDigest Buffer (MBI Fermentas)	
Nuclease-free water (MBI Fermentas)	
T4 DNA Ligase (Invitrogen)	
5x T4 DNA Ligase Buffer (Invitrogen)	250 mM Tris-HCl (pH 7.6), 50 mM $MgCl_2$, 5 mM ATP, 5 mM DTT, 25% (w/v) PEG
Cloning	
Cloning vector	pLL10 (pBluescript-based, (*142*))
Competent cells (Invitrogen)	One Shot® TOP10 Chemically Competent *E. coli*
LB agar (Invitrogen)	imMedia™ Amp Agar
Purification of linearized plasmid	
Proteinase K (Promega)	> 30 u/mg
Sodium dodecylsulphate/ SDS (Sigma-Aldrich)	10% stock solution
Phenol-chloroform-isoamylalcohol 25:24:1 (Sigma-Aldrich)	saturated with 10 mM Tris, pH 8.0, 1 mM EDTA
Chloroform (Merck)	
Isopropanol (Lach-ner)	
DEPC-treated water	0.1% diethylpyrocarbonate in water, autoclaved
RNA electrophoresis	
Agarose (Invitrogen)	
6x RNA loading dye	60% glycerol, 10 mM Tris-HCl (pH 7.6), 60 mM EDTA, 0.03% Bromophenol Blue, 0.03% Xylene Cyanol FF
RNA Ladder High Range (MBI Fermentas)	
PCR Ethidium bromide (Top-Bio)	10 mg/ml stock solution
quantitative PCR	
2x Fast start Universal SYBR Green Master (Roche)	FastStart Taq DNA Polymerase, Reaction Buffer, dNTPs, SYBR Green I, reference dye

3.2 Kits

Table 6: List of used kits

purpose	kit	manufacturer
Borrelia viability monitoring	LIVE/DEAD® *Bac*Light™ Bacterial Viability Kit	Molecular Probes
Gel purification of PCR product	QIAquick Gel Extraction Kit	Qiagen
Purification of PCR product	QIAquick PCR Purification Kit	Qiagen
Plasmid purification	QIAprep Spin Miniprep Kit	Qiagen
ssRNA synthesis	MEGAscript® T7 Kit	Ambion
ssRNA purification	MEGAclear™ Kit	Ambion
RNA isolation	NucleoSpin RNA II	Macherey-Nagel
cDNA synthesis	Transcriptor High Fidelity cDNA Synthesis Kit	Roche

3.3 Primers

Table 7: List of used primers (Generi Biotech, Hradec Králové, Czech Republic). The sites for restriction enzyme digestion are marked in bold.

name	sequence 5'-3'	annealing	amplicon
Salp25D F	CACCATGGGTCCCCTGAACCTCGGC	50°C	666 bp
Salp25D R	TCAGTCCATGGTTGTTCGGAGGT	50°C	
Salp25D RNAi F	AT**CTCGAG**GAAGGGTGTCAAGCTCATCG	60°C	487 bp
Salp25D RNAi R	AT**TCTAGA**GTCCATGGTTGTTCGGAGG	60°C	
Salp25D KD-F	GATCGACTTCCACGAATGG	55°C	123 bp
Salp25D KD-R	TTTTGAAAGACGTGGTGCAG	55°C	
actin-like F1	CGTCTGGATCGGCGGCTCTAT	55°C	530 bp
actin-like R1	ACGCGCACTCTTTTCCACAATCTC	55°C	
actin qRT-F	GATCATGTTCGAGACCTTCA	60°C	92 bp
actin qRT-R	CGATACCCGTGGTACGA	60°C	

3.4 Ticks

Ixodes ricinus adult non-engorged females were used for the experiments. The ticks were collected by flagging method in the forest locality near České Budějovice and kept at the tick rearing facility of the Biology Centre, Institute of Parasitology, Academy of Sciences of the Czech Republic.

4 METHODS

4.1 Bioinformatic analysis

Protein sequence of Salp25D was compared with GenBank database using BLASTp search (available on the website http://blast.ncbi.nlm.nih.gov). A multiple sequence alignment of 1-cysteine peroxiredoxins within tick species, and an interspecies alignment were done with Clustal Omega (http://www.ebi.ac.uk/Tools/msa/clustalo/).

4.2 Verification of Salp25D insert in the expression vector

The presence of Salp25D insert in the expression vector was confirmed by PCR with Salp25D F/R specific primers. One reaction (20 µl) consisted of 10 µl 2x PCR master mix, 1 µl 10 µM forward primer, 1 µl 10 µM reverse primer, 1 µl template DNA (c = 50 ng/µl) and 7 µl PCR water. The amplification proceeded according to the program summarized in Table 8. The PCR product was analyzed by DNA electrophoresis in 1% agarose gel at 100 V for 30 min. A 100 bp DNA marker was used to verify the size of the insert.

Table 8: The PCR program for Salp25D amplification.

step		temperature	time
1	initial denaturation	95°C	5 min
2	denaturation	95°C	30 s
3	primer annealing	50°C	30 s
4	primer extension	72°C	1 min
5	final extension	72°C	10 min
30x repeat step 2 to 4			

4.3 Production of recombinant protein in a bacterial system

4.3.1 Transformation of competent E. coli cells with the expression vector

One vial of BL21 Star™ (DE3) cells was thawed on ice. 1 µl of plasmid DNA (c = 50 ng/µl) was added to the vial and stirred gently. The mixture was incubated for 30 min. on ice and then heat-shocked for 30 s at 42°C. 250 µl room temperature-equilibrated S.O.C. medium were added and the vial was shaken (200 rpm) for 30 min. at 37°C. The whole transformation reaction was transferred into 10 ml sterile LB medium with ampicillin (final c = 50 mg/ml) and grown overnight at 37°C with shaking.

4.3.2 Pilot expression – time course monitoring

Fresh LB medium containing ampicillin was inoculated with overnight culture in a volume ratio 20:1 and grown until optical density reached 0.5-0.8 (2h). 1 ml of non-induced culture

was taken as a zero point sample. After IPTG was added to the culture (c = 1mM), 1 ml aliquot was taken every hour in 5-hour period. The samples were centrifuged at maximum speed for 30s, supernatant was aspirated and the pellets were dissolved in 100 µl TE buffer (pH 8). Afterwards, they were analyzed using SDS-PAGE.

4.3.3 Optimization of induction temperature

Expression of Salp25D was carried out at two different temperatures. The procedures were identical, except the cells were cultured at 37°C and at 30°C, respectively.

4.3.4 Large-scale expression of Salp25D

After optimization of the expression conditions, the large-scale expression of the target protein was performed. The bacteria were grown in a volume of 200 ml of LB medium with ampicillin. Induction time for the expression was 3 hours and the temperature was kept at 30°C. The cultured cells were centrifuged at 4000 rpm at 4°C for 20 min. Pellets were stored in -20°C until the purification step.

4.4 Purification of recombinant protein

Recombinant Salp25D (rSalp25D) carrying hexahistidine-tag was purified using nickel affinity chromatography. Purification was done under native conditions.

4.4.1 Preparation of E. coli lysate

The bacterial pellets were resuspended in lysis buffer (5 ml/1 g cells). Protease inhibitor cocktail (50 µl/1g cells) and lysozyme (1 mg/1 g cells) were added. Mixture was incubated on ice for 30 min and then sonicated at 20 kHz in 8 cycles per 10 s with 20 s cooling periods. After centrifugation at 10 000 g at 4°C for 20 min, supernatant was saved for further use.

4.4.2 Purification on Ni-NTA column

Ni-NTA agarose slurry was transferred into a plastic column (1 ml 50% resin/4 ml cell lysate). The beads were rinsed with distilled water (1x 5 ml) and further equilibrated with lysis buffer (2x 2 ml). The cell lysate was applied to the column and left to bind at 4°C overnight with shaking on a rotary shaker. Next day, the flow-through fraction was collected. The resin was washed five times with 5 ml of washing buffer and the protein was eluted five times with 0.5 ml of elution buffer. A 20 µl aliquot was removed from each fraction and analyzed by SDS-PAGE.

4.5 SDS-PAGE analysis

SDS-polyacrylamide gel consisting of 12% resolving gel and 4% stacking gel was prepared according to Laemmli method. Meanwhile, 14 µl of each protein sample were mixed with 5 µl 4x loading buffer and 1 µl 20x reducing agent. The mixture was incubated at 99°C for 5 min and then centrifuged at maximum speed for 10 min. The samples were loaded on the gel and the electrophoresis was run in Hoefer SE250 Mighty Small II at 20 mA/gel for 1.5 h. Proteins were visualized by staining in PageBlue staining solution followed by washing in distilled water.

4.6 Dialysis, concentration

The eluted protein was transferred to cellulose dialysis tube (12 kDa cutoff, Sigma-Aldrich) and dialyzed against 1000x sample volume of 1x PBS (pH 7.4). After 4 hours, buffer was exchanged for a fresh one and the dialysis continued overnight.

Final concentration of protein was measured using Nanophotometer P300 (Implen). When needed, the protein was further concentrated in Vivaspin 2 (10 kDa cutoff, Sartorius) vertical membrane concentrator. Protein samples were stored at -20°C in 100-200 µl aliquots.

4.7 Western blotting

Protein samples were transferred from unstained polyacrylamide gel onto a PVDF membrane (Immobilon-P, Merck Millipore). Blotting was performed at 250 mA for 1.5 h in Genie apparatus (Idea Scientific). Detection of the target protein was done using Ni-NTA HRP conjugates (Qiagen). In brief, membrane was washed 2x 10 min with TBS, incubated for 1 h in TBS supplemented with 3% BSA to block the unspecific binding, washed 3x 10 min with TBS-Tween and stained for 5 min in HRP staining solution. Chromogenic reaction was stopped by rinsing the membrane in water. The membrane was photographed immediately after drying.

4.8 Functional assays

4.8.1 DNA nicking assay

Thiol-dependent metal-ion catalyzed oxidation system (MCO) consisting of Fe^{3+}, O_2, DTT is able to produce harmful hydroxyl radicals (*143*) in a series of reactions (reactions 20-23). These can damage DNA by forming single-stranded breaks that mediate a switch of the

supercoiled form of DNA to the open-circular form. The nicking effect can be observed on an agarose gel.

20. $RSH + 2\,Fe^{3+} \rightarrow 2\,RS^{\bullet} + 2\,Fe^{2+} + 2H+$
21. $Fe^{2+} + O_2 \rightarrow O_2^{\bullet -} + Fe^{3+}$
22. $Fe^{2+} + 2H^{+} + O_2^{\bullet -} \rightarrow H_2O_2$
23. $H_2O_2 + Fe^{2+} \rightarrow Fe^{3+} + OH^{\bullet} + OH^{-}$

The experiment was performed essentially as described by Lim and colleagues (*144*). The reaction mixtures (total volume: 50µl) consisted of 3 µM $FeCl_3$, 0.1 mM EDTA, 10 mM DTT and increasing concentrations of rSalp25D in 50 mM HEPES buffer. $FeCl_3$ was pre-incubated with EDTA, as was rSalp25D with DTT, for 10 min at 37°C. The two pre-incubated samples were mixed and the reaction was incubated at 37°C for 30 min. Then, 200 ng of pBR322 supercoiled plasmid DNA was added to each reaction mixture and incubated for another 2.5 h. Half of the mixture was taken and the rest was further incubated for 1.5 h. The incubated samples were mixed with 6x loading dye containing SYBR Gold nucleic acid stain and loaded onto a 0,8% agarose gel. Electrophoresis was run at 100V for 30 min.

4.8.2 Borrelia viability assay – LIVE/DEAD

Viability of *B. burgdorferi* in presence of oxidative stress and the effect of Salp25D on their survival were investigated. Live and dead spirochetes were distinguished by fluorescent staining of the nucleic acid by two different dyes. SYTO9 green fluorescent dye stains nucleic acids of all bacteria, whereas the red colored propidium iodide can only penetrate bacteria with damaged membranes, in which case it competes for DNA binding with SYTO9.

Hydroxyl radicals were generated by metal-ion catalyzed oxidation system as specified above. 100 µg/ml rSalp25D was added and the reaction was incubated at 37°C for 1h. After addition of 50 µl *in vitro* grown spirochetes (*B. burgdorferi* s.s., strain ZS7, 10^7-10^8/ml), the reaction was incubated at 37°C for another 1.5 h. Afterwards, 0.3 µl of 1:1 mixture of fluorescent dyes from LIVE/DEAD BacLight Bacterial Viability Kit was added and the reaction was incubated in dark for 15 min. 3.5 µl of the reaction were examined on Olympus FluoView FV10i Confocal Microscope (magnification 60x). Live and dead spirochetes were counted in 10 different fields and averaged.

4.8.3 Borrelia viability assay – FACS

Fluorescence activated cell sorting (FACS) was used to determine the counts of viable and dead borrelia. The method was based on staining of cells with propidium iodide and determining the proportion of dead spirochetes to the total number of spirochetes in the experiment.

Hydroxyl radicals were generated as specified above. Total reaction volume was 300 µl, containing 100 µg/ml rSalp25D. After incubation for 45 min, 10 µl *in vitro* grown spirochetes (*B. burgdorferi* s.s., strain ZS7, 10^7-10^8/ml) was added and incubation continued at 37°C for 1.5 h. Then, 2 µl propidium iodide solution was added to the reaction and incubated in dark for 15 min. The mixture was subjected to analysis with BD FACS Canto II device (total events: 20 000, flow rate: slow).

4.8.4 Assay for glutathione peroxidase (GPx) activity

Glutathione peroxidase catalyzes reduction of peroxide to hydroxide (or to H_2O) and oxidation of glutathione in a coupled reaction. NADPH is needed as a reductant to recover glutathione in its reduced form. This second reaction is catalyzed by another enzyme – glutathione reductase (Figure 9). The reaction was prepared *in vitro* to detect possible glutathione peroxidase activity of rSalp25D.

The reaction was carried out in 1 ml solution containing 50 mM potassium phosphate buffer (pH 7), 1 mM EDTA, 1mM GSH, 1 unit GR and 100-200 µg/ml rSalp25D. The reaction was incubated for 5 min, 0.25 mM NADPH was added and the incubation continued for 5 min. The reaction was initiated by addition of 0.5 mM hydrogen peroxide and the decrease of absorbance at 340 nm was measured in a cuvette using Nanophotometer P300 (Implen).

The same reaction was also run in 200 µl volume in a microtiter plate. Here, three different concentrations of hydrogen peroxide were tested (0.1 mM, 0.25 mM and 0.5 mM). The course of reaction was monitored for by TECAN Infinite M200 spectrophotometer.

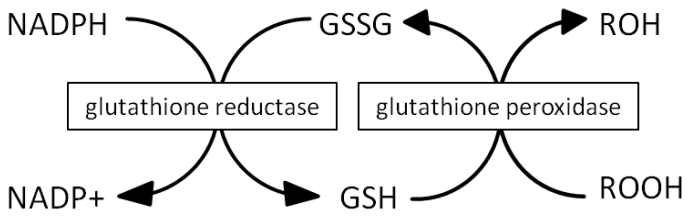

Figure 9: Scheme of the coupled redox reactions involving glutathione, glutathione peroxidase and glutathione reductase. Reaction depends on reducing equivalent donated by NADPH. Conversion of NADPH to $NADP^+$ can be measured spectophotometrically.

4.9 RNA interference

4.9.1 Preparation of dsRNA

4.9.1.1 PCR with primers for RNAi

Primers with restriction sites for XhoI and XbaI enzymes and AT overhangs were designed. Optimal annealing temperature of primers was determined using gradient PCR (GenePro, Bioer). One reaction (20 µl) consisted of 10 µl 2x PCR master mix, 1 µl 10 µM Salp25D RNAi F primer, 1 µl 10 µM Salp25D RNAi R primer, 1 µl template DNA (c = 100 ng/µl) and 7 µl PCR water. The program was essentially the same as in Table 7, but four different temperatures were used for the annealing – 50, 55, 60 and 62°C. The band with optimal amplification results was excised from agarose gel and purified using QIAquick Gel Extraction Kit (Qiagen).

4.9.1.2 Restriction of PCR product and plasmid pLL10

Both the PCR product and pLL10 plasmid (c = 132 ng/µl) were digested with XhoI and XbaI restriction enzymes. Components of the reactions are depicted in Table 9. Reactions were incubated at 37°C for 1,5 h. Digested plasmid and PCR product were purified with QIAquick Gel Extraction Kit and QIAquick PCR Purification Kit, respectively.

Table 9: Digestion of PCR product and plasmid.

component	volume (µl)	
	pLL10 plasmid	PCR product
FastDigest buffer 10x	3	3
FastDigest XhoI	1	1
FastDigest XbaI	1	1
DNA	3 (400 ng)	20 (whole reaction)
nuclease-free water	22	5
total	30	30

4.9.1.3 Ligation into pLL10 vector

The components of the ligation reaction (Table 10) were mixed and incubated for 1 hour at room temperature and then left overnight at 4°C.

Table 10: Ligation reaction.

component	volume (µl)
T4 ligase (1U/µl)	1
T4 ligase buffer 5x	2
digested plasmid	2
digested PCR product	2
nuclease-free water	3
total	10

4.9.1.4 Transformation, selection of positive clones

TOP10 Competent cells were transformed with the ligation product. The entire volume of ligation reaction was mixed with one vial of TOP10 cells and incubated on ice for 30 min. The cells were heat-shocked for at 42°C for 1 min and then incubated on ice for 2 min. 500 µl of S.O.C. medium was added and the mixture was shaken at 200 rpm and 37°C. The mixture was spread on pre-warmed agar plates in two different concentrations to allow the optimal colonies separation. Plates were incubated at 37°C for 12 hours. Fifteen colonies were picked from one plate and PCR with Salp25D RNAi primers was performed to identify the colonies with the insert. From colonies that contained the ligation product, four were randomly chosen and grown each in 30 ml LB medium (with ampicillin) overnight. Overnight cultures were divided into 5 ml aliquots and centrifuged at maximum speed for 10 min. Plasmids were purified from the cell pellets using QIAprep Spin Miniprep Kit and sequenced. Subsequently, a glycerol stock was prepared from one of the cultures by mixing 750 µl cultured cells with 250 µl sterile glycerol.

At the same time, overnight culture was grown from a glycerol stock of TOP10 cells carrying plasmid with GFP insert (provided by the laboratory of doctor Kopáček). GFP served as a negative control during RNA interference. Plasmid was purified using QIAprep Spin Miniprep Kit.

4.9.1.5 Restriction of purified plasmid

Plasmids with Salp25D and GFP (10 µg/50 µl reaction) were mixed with restriction enzymes as specified in Table 11. Reaction was incubated at 37°C for 1h.

Table 11: Restriction of purified plasmid.

component	volume (µl)			
	Salp25D - XhoI	**Salp25D - XbaI**	**GFP - ApaI**	**GFP - XbaI**
plasmid (10 µg)	30	25	30	30
10x FastDigest Buffer	5	5	5	5
FastDigest ApaI	-	-	6	-
FastDigest XbaI	-	6	-	6
FastDigest XhoI	6	-	-	-
nuclease-free water	9	14	9	9
total	50	50	50	50

4.9.1.6 Purification of digested plasmid

The solution of proteinase K was prepared, containing 1µl of proteinase K (20 µg/µl) in 150 µl 10 mM Tris-HCl and 2 mM $CaCl_2$. Twenty-five µl of the solution and 3.75 µl 10 % SDS was added into the restriction reactions, and incubated at 50°C for 30 min. The reaction content was extracted with 80 µl phenol:chloroform:isoamyl alcohol, vortexed vigorously and centrifuged at 13 000 rpm for 5 min. Aqueous phase was collected and extracted once more with 80 µl chloroform. After that, 56 µl isopropanol was added to aqueous phase, mixed by pipetting and incubated for 30 min at -20°C. The mixtures were centrifuged at 13000 rpm at 4°C for 30 min. Pelleted DNA was washed with 80 µl 75% ethanol in DEPC water, centrifuged for 8 min and the ethanol was removed. After complete drying, pellets were resuspended in 10 µl DEPC water and the concentration was checked.

4.9.1.7 Synthesis of ssRNA (in vitro transcription)

One microgram of linearized plasmid DNA was used for synthesis of RNA using the MEGAscript T7 Kit. Reaction components are specified in Table 12. The mixture was incubated at 37°C overnight. Newly synthesized RNA molecules were purified using MEGAclear Kit including the optional ammonium acetate precipitation step.

Table 12: *In vitro* transcription reaction.

component	volume (µl)			
	Salp25D - XhoI	**Salp25D - XbaI**	**GFP - ApaI**	**GFP - XbaI**
linearized plasmid(1µg)	4	4	4	5
nucleotides	4x 2	4x 2	4x 2	4x 2
10x buffer	2	2	2	2
enzyme mix	2	2	2	2
nuclease-free water	4	4	4	3
total	20	20	20	20

4.9.1.8 Synthesis of dsRNA

All RNAs were diluted to the final concentration 3 µg/µl. The sense and antisense strand of each RNA group (Salp25D, GFP) were mixed in ratio 1:1. Hybridization was initiated by immersing the samples into boiling water and continued for 12 hours. After that, the quality of produced ssRNAs and dsRNAs was checked by agarose gel electrophoresis. 10 µl RNA (1 µg) was mixed with 2µl loading dye supplied with the kit and loaded onto a 1% agarose gel in 1x TAE. Electrophoresis was run at 100V for 45 min. The gel was stained in 0,2 µg/ml EtBr solution and visualized under UV light.

4.9.2 Tick injection

A total number of 47 adult female ticks were divided into two groups – control GFP group (25 ticks) and Salp25D group (22 ticks). Ticks in each group were injected either with GFP dsRNA or with Salp25D dsRNA. The injection was carried out using Narishige MN-151 micromanipulator connected to Olympus KL1500 microscope. Double-stranded RNA was injected by glass needle between the coxa and trochanter of the 3rd leg (Figure 10) to get it into the hemolymph of the ticks. The ticks were activated by breathing CO_2 on them right after the injection, followed by overnight incubation at 17°C in humid conditions.

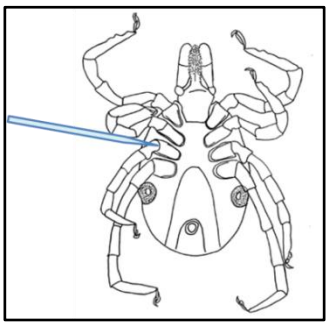

Figure 10: Site of dsRNA injection into the tick, picture reproduced from: http://www.zoologie.frasma.cz/mmp 0211 klepitkatci/klepitkatci web.html

4.9.3 Tick feeding and dissection

The ticks from both groups were fed separately on two guinea-pigs for 6 days. Eleven ticks of each group were picked and dissected. Salivary glands, ovaries and gut were separated and kept in a buffer for RNA isolation. Only ¼ of the gut tissue, properly rinsed with PBS (to get rid of the blood content), was taken for the further experiment.

4.9.4 Confirmation of gene silencing

4.9.4.1 Total RNA isolation

Total RNA was isolated from selected organs using NucleoSpin RNA II kit. The concentration was measured using Nanophotometer P300. Quality of extracted RNA was assessed on 1,2 % agarose gel in 1x TAE. Before loading on the gel, RNA was heated for 70°C for 1 min and then incubated on ice. The electrophoresis was run at 80 V for 1 hour.

4.9.4.2 cDNA synthesis

First strand cDNA was prepared using Transcriptor High Fidelity cDNA Synthesis Kit. Standard procedure for quantitative RT-PCR, which uses random hexamer primers, was selected. Obtained cDNA was diluted 10x and its quality was verified by qualitative PCR with tick actin primers (actin-like F1 and R1) as a housekeeping control.

4.9.4.3 Quantitative PCR

The PCR reaction was carried in LightCycler 480 (Roche) instrument. Reactions (Table 13) were pipetted into a microplate for fluorescence. Actin from *I. ricinus* was chosen as a reference gene. All samples were prepared in duplicates. The program used for amplification is presented in Table 14. The C_T values were collected and used for relative quantification of Salp25D expression in the organs of knock-down and control group.

Table 13: Quantitative PCR reaction setup.

component	volume (µl)
FastStart Universal Sybr Green Master 2x	12,5
10 µM primer F (Salp25D KD-F or actin qRT-F)	1
10 µM primer R (Salp25D KD-R or actin qRT-R)	1
cDNA (10x diluted)	5
PCR water	5,5
total	25

Table 14: Program for quantitative PCR.

step		temperature	time
1	initial denaturation	95°C	5 min
2	denaturation	95°C	10 s
3	primer annealing	60°C	10 s
4	primer extension	72°C	10 s
45x repeat step 2 to 4			

5 RESULTS

5.1 Bioinformatic analysis

Protein BLAST search was performed using Salp25D from *I. ricinus* as a query sequence. Salp25D showed similarity to peroxiredoxins with one conserved cysteine (often called Prx6). The highest similarity was observed with other hard and soft tick species, ranging from 90 to 99% identity at protein level. More than 60% AA identity with *I. ricinus* Salp25D was detected in multiple invertebrate and vertebrate species. Similarity with plants or protists was generally lower, around 50% (Table 15).

Multiple sequence alignments are provided in the Appendix section (A and B). There is a high homology between known Prxs of ticks. On the other hand, homology of random organisms picked across the phyla is not so pronounced, but the 1-Cys Prx motif remains conserved.

Table 15: Similarity of various 1-Cys Prx with Salp25D from *Ixodes ricinus* (blastp tool).

organism	trivial name	GenBank number	AA identity (%)
Ixodes scapularis	black-legged tick	AF209911	99
Haemaphysalis longicornis	bush tick	AB038382	91
Metaseiulus occidentalis	predatory mite	XM_003748181	83
Strongylocentrotus intermedius	sea urchin	HM208171	67
Drosophila melanogaster	fruit fly	AF311878	64
Arenicola marina	lugworm	DQ059567	62
Bos taurus	bovine	NM_174643	62
Homo sapiens	human	D14662	60
Plasmodium falciparum	malaria parasite	AB020595	50
Arabidopsis thaliana	mouse-ear cress	F21D18.15	49

5.2 Salp25D insert in the expression vector

Presence of the Salp25D insert in the expression vector was confirmed by PCR (Figure 11). The appropriate construct was further used for the expression of target protein in a bacterial system.

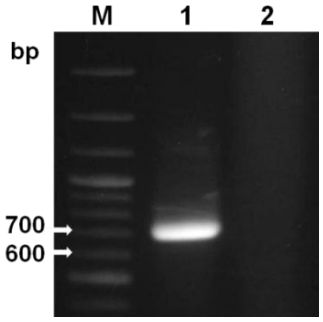

Figure 11: Salp25D insert (666 bp) in the expression vector. M= 100bp marker, 1= Salp25D insert, 2= negative control.

5.3 Production of recombinant protein in a bacterial system

5.3.1 Pilot expression – time course monitoring, temperature optimization

Salp25D was expressed as a 6xHis-tagged fusion protein of 27.5 kDa. In order to determine the optimal conditions for the expression, induction process was monitored for 5 hours at two different culturing temperatures (30°C and 37°C). It was revealed that the protein was successfully expressed in both cases. At 30°C, the expression increased gradually with time (Figure 12), whereas at 37°C, the expression was relatively constant at every time point (Figure 13). According to these results, 3 hours were estimated as the optimal induction time for the culture growth at 30°C and 2 hours for the culture at 37°C. Maximal induction times were avoided to prevent the accumulation of protein side-products. Expression at 30°C with two-hour induction was selected for further experiments.

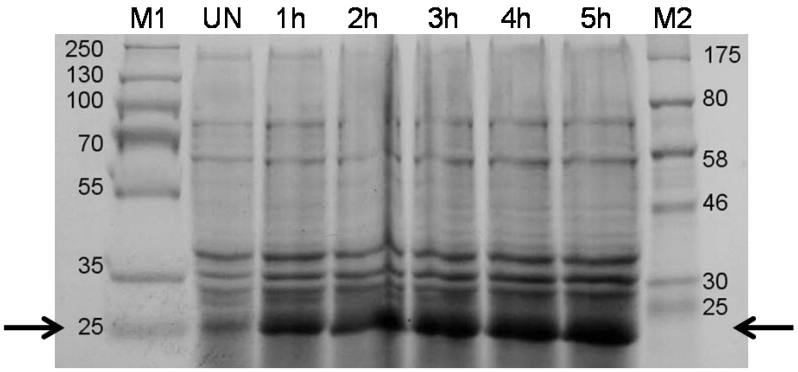

Figure 12: SDS-PAGE analysis of pilot expression of Salp25D at 30°C. M1 = PageRuler Plus Prestained Protein Ladder, UN = uninduced sample, 1h- 5h = samples after induction, M2 = Prestained Protein Marker. The target protein is marked with black arrows.

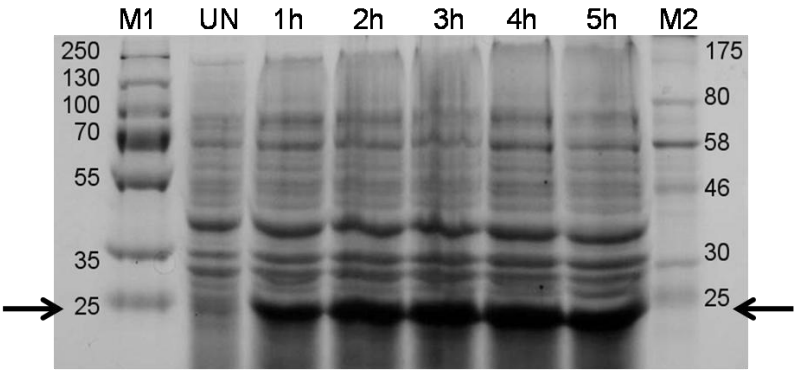

Figure 13: SDS-PAGE analysis of pilot expression of Salp25D at 37°C. M1 = PageRuler Plus Prestained Protein Ladder, UN = uninduced sample, 1h- 5h = samples after induction, M2 = Prestained Protein Marker. The target protein is marked with black arrows.

5.3.2 Protein purification

The recombinant 6xHis-tagged protein was purified using Ni-NTA agarose. The process was optimized by increasing the concentration of imidazol in the washing buffer from 20 mM to

50 mM as well as by increasing the number of washing fractions (3→5) and washing buffer volume (4 ml → 5ml). Optimization procedure removed vast majority of non-specific proteins from the sample (Figure 14), in comparison with the initial expression experiment (Figure 15).

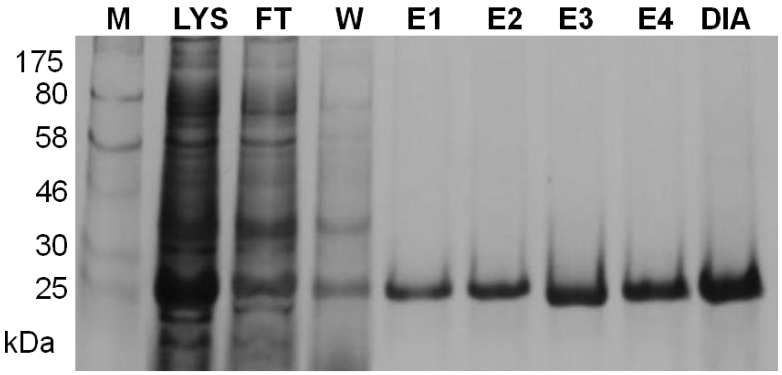

Figure 14: SDS-PAGE analysis of Salp25D expression after optimization. M = protein marker, LYS = cell lysate, FT= flow-through fraction, W = washing fraction, E1-E4 = elution fractions, DIA = protein after dialysis.

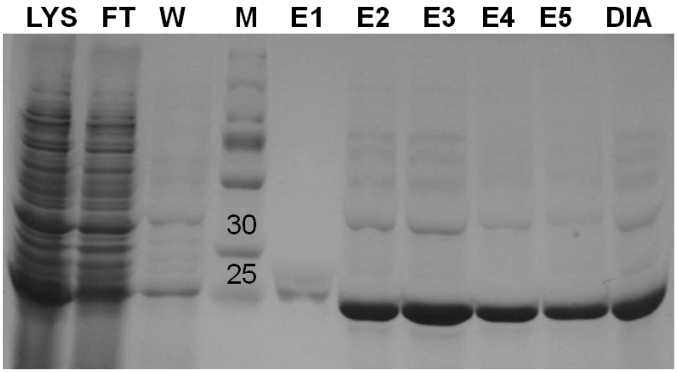

Figure 15: SDS-PAGE analysis of Salp25D expression. LYS = cell lysate, FT= flow-through fraction, W = washing fraction, M = protein marker, E1-E4 = elution fractions, DIA = protein after dialysis.

5.3.3 Western blot

The presence of target fusion protein in the purified samples was confirmed by western blot with specific Ni-NTA HRP conjugates binding the histidine tag of the recombinant protein. The protein was detected in all elution fractions as well as in dialyzed sample (Figure 16).

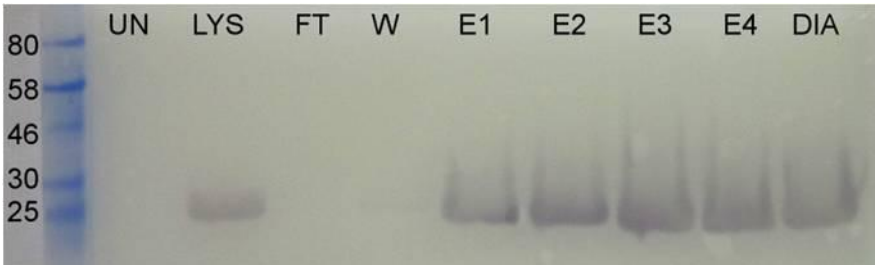

Figure 16: Western blot detection of His-tagged protein with Ni-NTA HRP Conjugates. UN = uninduced sample, LYS = cell lysate, FT= flow-through fraction, E1-E4 = elution fractions, DIA = protein after dialysis.

5.4 Functional assays

5.4.1 DNA nicking assay

The ability of rSalp25D to protect DNA from hydroxyl radical mediated damage was examined. We observed preservation of supercoiled form of DNA in case of incomplete MCO system and a significant DNA nicking effect of full MCO system. With increasing concentration of rSalp25D in the reaction, the DNA was prevented from nicking (Figure 17). We also noticed that the longer incubation time of DNA with hydroxyl radicals needs higher concentrations of rSalp25D to keep the rescuing capacity. In the case of 2,5 h incubation, supercoiled form was protected from the concentration 50 μg/ml of rSalp25D (Figure 17), whereas at 4 h incubation (Figure 18), the preservation of supercoiled form started at Salp25D concentration of 100 μg/ml.

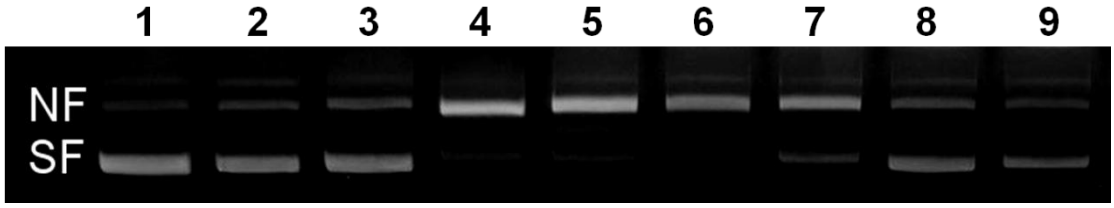

Figure 17: Oxidative stress cause nicking of supercoiled DNA. Incubation of metal-ion catalyzed system (MCO) with plasmid DNA for 2,5 h. NF = nicked form, SF = supercoiled form, 1 = plasmid pBR322, 2 = incomplete MCO system (Fe3+), 3 = incomplete MCO system (DTT), 4 = full MCO, 5 = MCO + rSalp25D 10 μg/ml, 6 = MCO+ rSalp25D 20 μg/ml, 7 = MCO + rSalp25D 50 μg/ml, 8 = MCO + rSalp25D 100 μg/ml, 9 = MCO + rSalp25D 200 μg/ml.

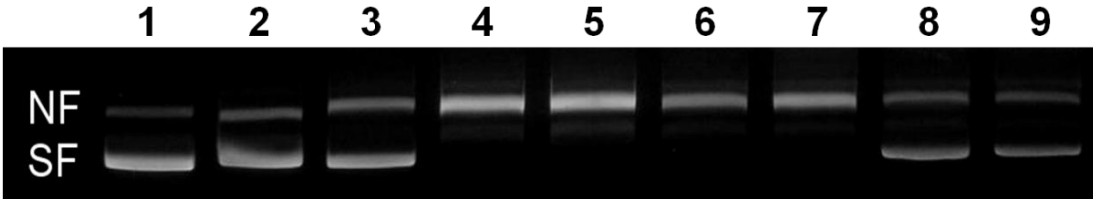

Figure 18: Oxidative stress cause nicking of supercoiled DNA. Incubation of metal-ion catalyzed system (MCO) with plasmid DNA for 4 h. NF = nicked form, SF = supercoiled form, 1 = plasmid pBR322, 2 = incomplete MCO system (Fe3+), 3 = incomplete MCO system (DTT), 4 = full MCO, 5= MCO + rSalp25D 10 μg/ml, 6 = MCO+ rSalp25D 20 μg/ml, 7 = MCO + rSalp25D 50 μg/ml, 8 = MCO + rSalp25D 100 μg/ml, 9 = MCO + rSalp25D 200 μg/ml.

5.4.2 Borrelia viability assay – LIVE/DEAD

Ratio of live (green) and dead (red) spirochetes was determined using confocal microscope. Borrelia in three experimental groups were counted in 10 random fields and averaged. Control group of borrelia contained 77% live spirochetes. Under conditions of oxidative stress, the number of dead borrelia slightly outnumbered the live spirochetes (45.9% vs. 54.1%). When rSalp25D was present in the reaction, more borrelia survived the oxidative

stress conditions (62.9% vs. 37.1%). The results are summarized in Graph 1. A representative image was taken for each of the samples at 60x magnification (Figure 19) and processed with FV10 ASW Viewer 1.7 software.

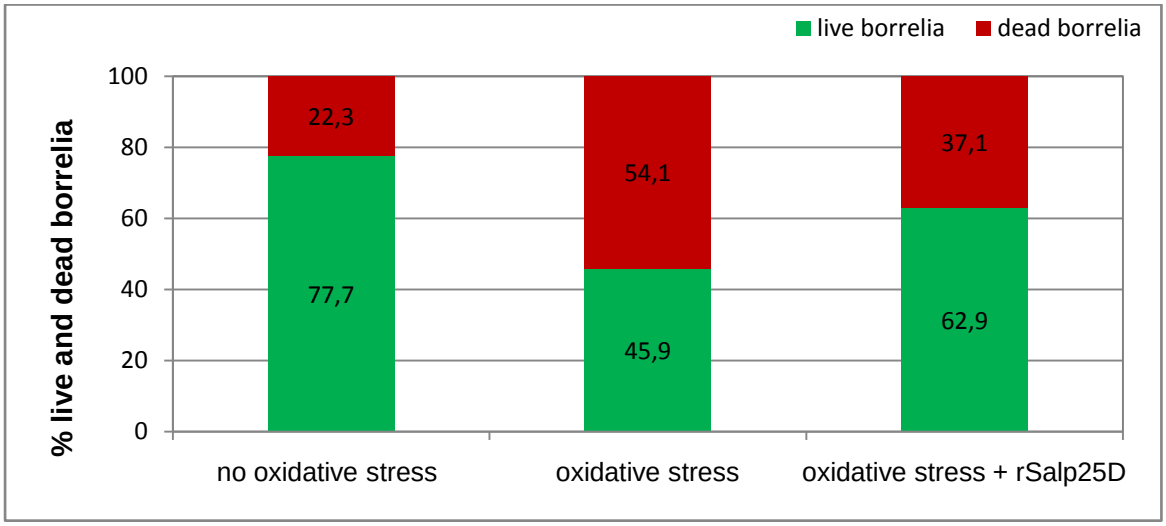

Graph 1: Proportions of live and dead borrelia counted using Olympus FluoView FV10i at 60x magnification. Spirochetes were counted in three experimental groups: no oxidative stress = borrelia in PBS, oxidative stress = borrelia in MCO system, oxidative stress+ rSalp25D = borrelia in MCO system + 100 µg/ml rSalp25D.

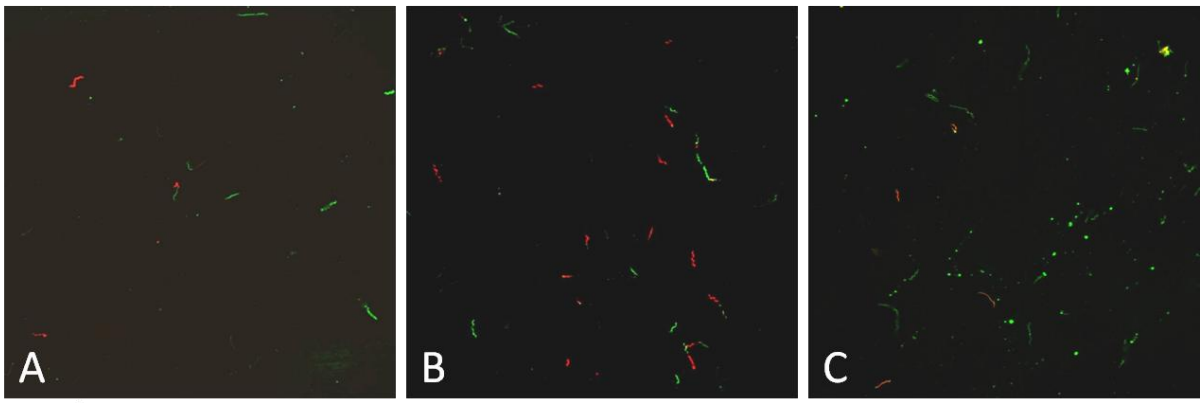

Figure 19: A = control - borrelia in PBS, B - Borrelia in MCO system, C – Borrelia in MCO system + 100 µg/ml rSalp25D, counted using Olympus FluoView FV10i at 60x magnification.

5.4.3 Borrelia viability assay – FACS

Percentage of dead borrelia killed by oxidative stress was also counted by FACS method. From the total number of cells counted (20 000), only 9.2 % of spirochetes were dead in the control group without MCO system. Under oxidative stress, the number increased up to 63.2%. In the presence of rSalp25D (100 µg/ml), the survival of borrelia was higher and only 18.9% of cells were dead. Figure 20 displays the counts of cells showing PI fluorescence, with highlighted subpopulation of dead cells (fluorescence intensity above 10^3). The results of the analysis are summarized in Graph 2.

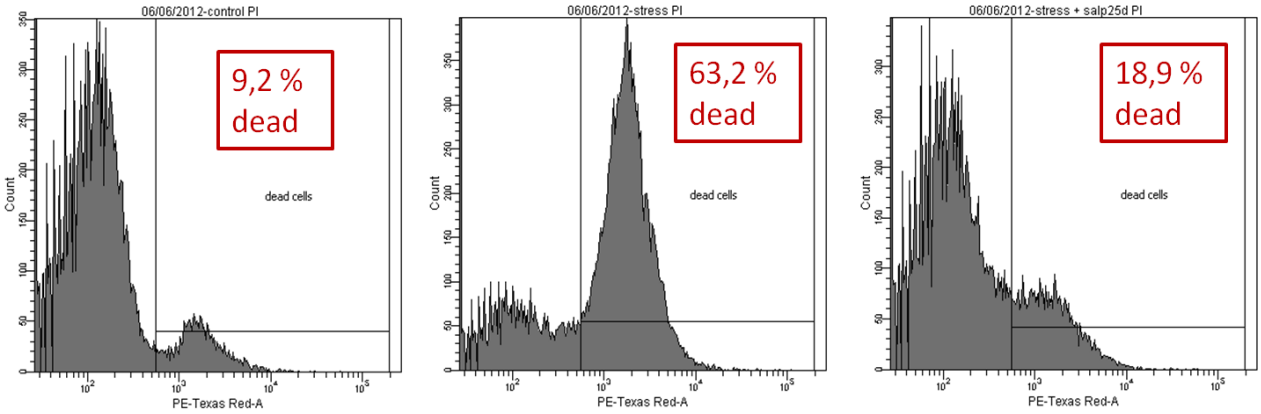

Figure 20: Fluorescence activated cell sorting - graphs of cell count vs. propidium iodide (same λ as PE-Texas Red) fluorescence. Subpopulation of dead cells is marked.

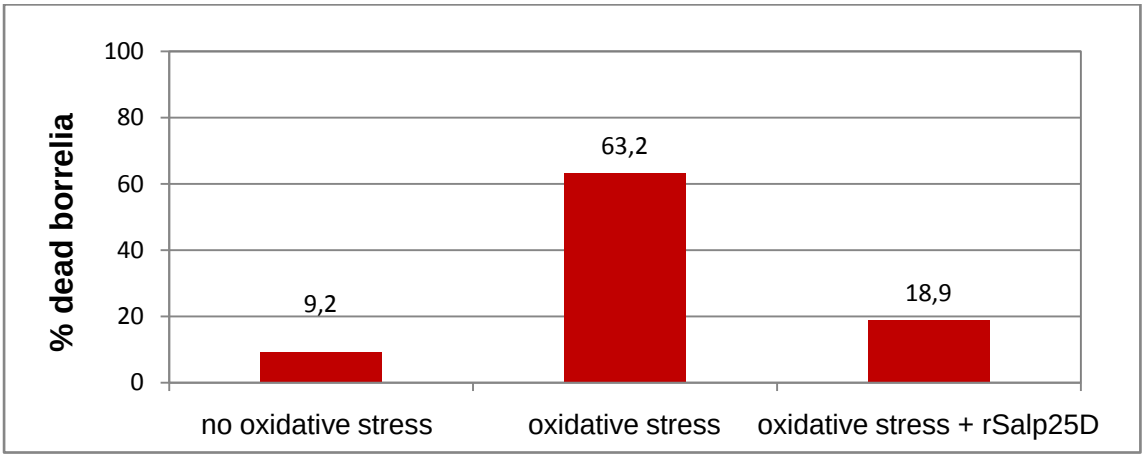

Graph 2: Percentage of dead borrelia counted by BD FACS Canto II. Spirochetes were counted in three experimental groups: no oxidative stress = borrelia in HEPES buffer, oxidative stress = borrelia in MCO system, oxidative stress+ rSalp25D = borrelia in MCO system + 100 µg/ml rSalp25D.

5.4.4 Assay for GPx activity

Reduced glutathione was tested as a substrate for the reaction catalyzed by rSalp25D. The reaction was performed both in a cuvette (1 ml reaction volume) and in a microplate (200 µl reaction volume). The depletion of NADPH was observed in the positive control with commercial GPx. Samples with rSalp25D did not show any decrease of absorbance in time and were comparable to negative control sample (Graph 3).

To rule out the possible inhibitory effect of high peroxide concentrations, three different concentrations of hydrogen peroxide were used (0.1, 0.25 and 0.5 mM). The change of concentration had affected the decrease of absorbance in positive control, but not in the experimental samples. The decrease of absorbance of rSalp25D containing sample was comparable to negative control (Figure 21).

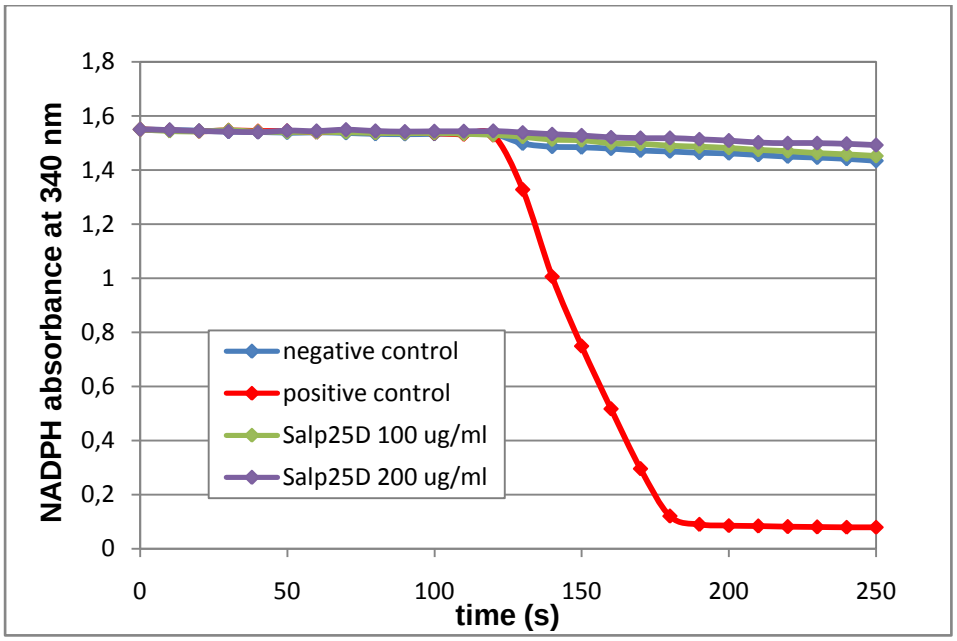

Graph 3: Detemination of the GPx activity of rSalp25D by monitoring the absorbance of NADPH at 340 nm. Negative control = reaction without enzyme, positive control = commercial GPx (Sigma-Aldrich). Kinetic cycle was measured by Nanophotometer P300. Initial absorbances were normalized to negative control. At time 120s, the reaction was initiated by addition of H_2O_2.

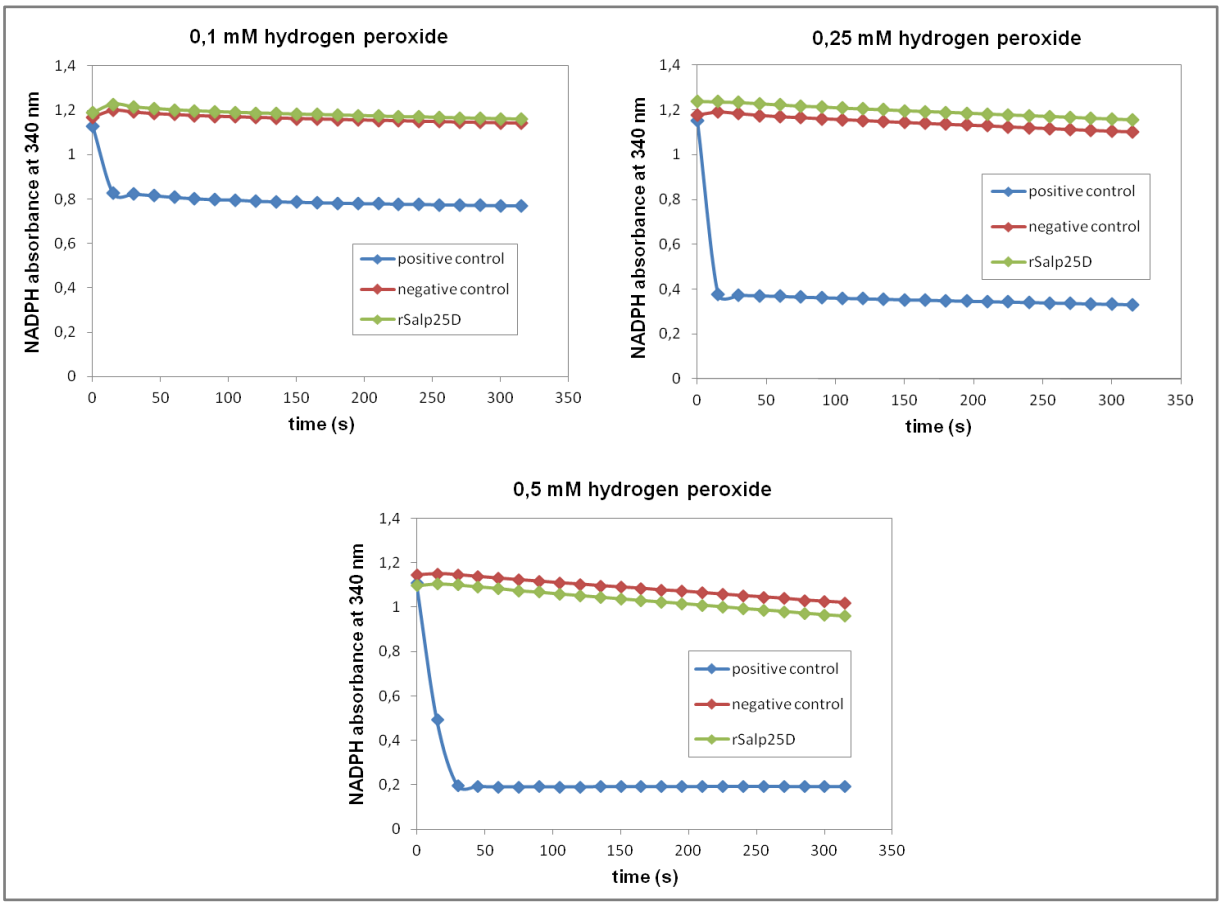

Figure 21: Effect of hydrogen peroxide concentration on the peroxidase activity of rSalp25D. Positive control = with commercial GPx, negative control = without rSalp25D enzyme, rSalp25D = 100 µg/ml enzyme.

5.5 RNA interference

5.5.1 dsRNA preparation

PCR with Salp25D primers for RNAi was performed. Amplification worked well within the whole temperature range (50 to 62°C). After purification of the target fragment (487 bp) from the gel, digestion, ligation and transformation, the screening was performed. All 15 picked colonies showed the uptake of Salp25 insert (Figure 22). Plasmid was then purified from the colonies 1, 6, 9 and 13. The presence of Salp25D insert was confirmed in all the samples by sequencing. Colony number 1 was chosen for further experiments.

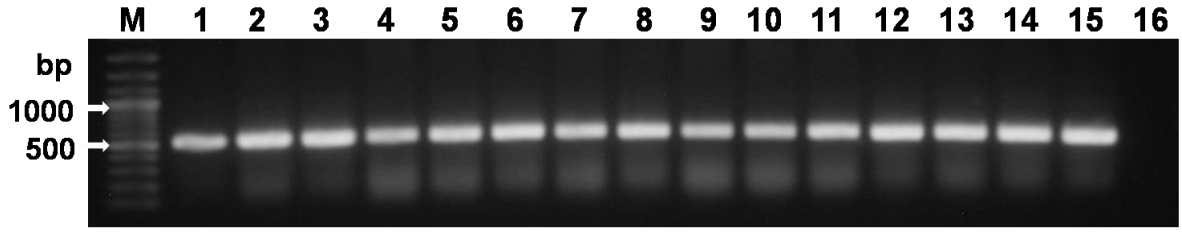

Figure 22: Result of PCR of 15 random colonies with Salp25D primers for RNAi (1-15). M = 100 bp marker, 16 = negative control.

Overnight cultures were grown from the glycerol stocks of cells containing Salp25D and GFP construct, and the plasmids were isolated from each culture. Due to the low concentration, plasmid DNA had to be further concentrated on MICRO-CENVAC evaporator (N-BIOTEK) to obtain at least 10 µg DNA in a volume of 30 µl. After the restriction, two types of linearized plasmids were produced for each group (Figure 23). Plasmids were used for *in vitro* transcription to ssRNAs (one sense and anti-sense strand per each group) which were further hybridized in pairs to yield dsRNA (Figure 23). Sufficient amount of good-quality dsRNA (3 µg/µl) was produced for each gene.

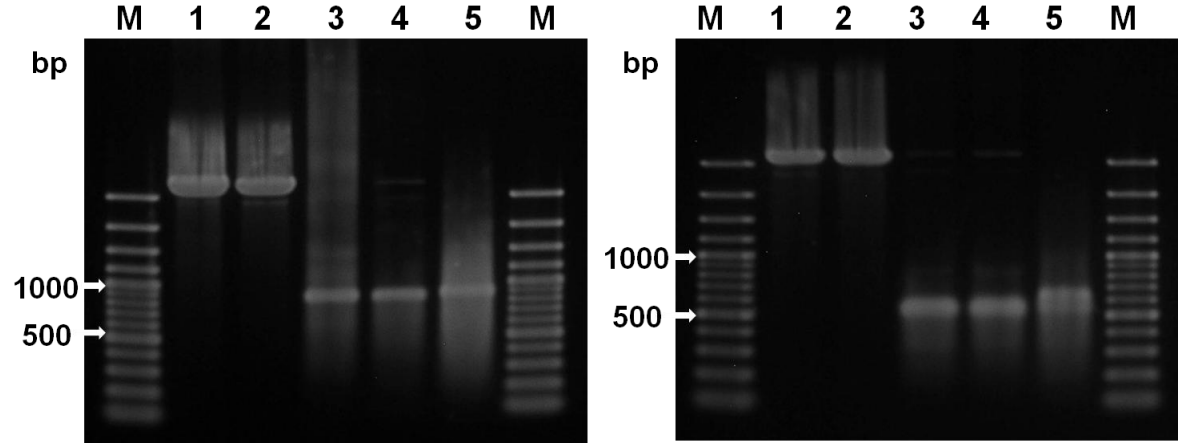

Figure 23: The course of procedure of dsRNA preparation. Left: preparation of GFP dsRNA. M = 100 bp marker, 1 = linearized plasmid ApaI, 2 = linearized plasmid XbaI, 3 = ssRNA ApaI, 4 = ssRNA XbaI, 5 = dsRNA GFP. Right: preparation of Salp25D RNA. M = 100 bp marker, 1 = linearized plasmid XhoI, 2 = linearized plasmid XbaI, 3 = ssRNA XhoI, 4 = ssRNA XbaI, 5 = dsRNA Salp25D.

5.5.2 Tick injection and feeding

Twenty-five tick females were injected with GFP dsRNA (control group) and twenty-two with Salp25D dsRNA (experimental group). Out of them, four ticks did not survive the injection in the control group. The rest of viable ticks were let to attach to two guinea-pigs (one for each group) together with the same amount of males and let feed for six days. Out of the total number, 13 ticks attached in the GFP group and 14 ticks in the Salp25D group.

Eleven ticks from each group were dissected. Total RNA was isolated from ovaries, salivary glands and gut using NucleoSpin RNA II kit. The quality of RNA was checked on agarose gel (Figure 24). There were no signs of degradation and the pattern corresponded to total RNA. The concentrations of isolated RNAs were measured and the samples were diluted with DEPC water in order to obtain equal concentrations in all samples (1μg). RNAs were reversely transcribed to cDNAs. To confirm the quality of the cDNAs, PCR reaction was done with primers for tick actin-like gene. Uniform amplification was observed in all samples (Figure 25).

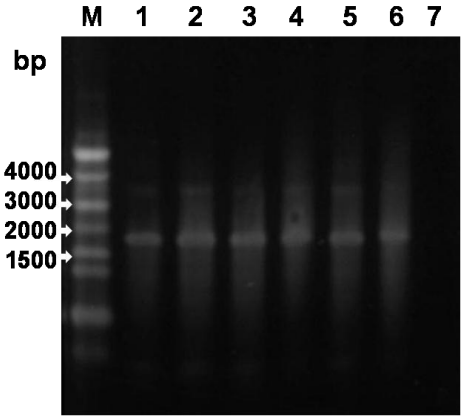

Figure 24: Total RNA on 1,2% agarose gel in TAE. M = RNA Ladder High Range, 1= Salp25D ovaries, 2 = Salp25D salivary glands, 3 = salp25D gut, 4 = GFP ovaries, 5= GFP salivary glands, 6 = GFP gut, 7 = negative control.

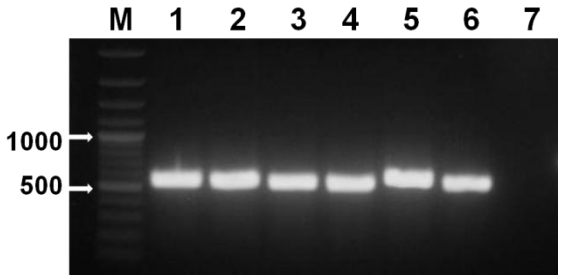

Figure 25: PCR with tick actin-like primers (amplicon 530 bp). M = 100 bp marker, 1 = Salp25D ovaries, 2 = Salp25D salivary glands, 3 = salp25D gut, 4 = GFP ovaries, 5 = GFP salivary glands, 6 = GFP gut. 7 = negative control.

5.5.3 Salp25D silencing

Optimal annealing temperature of primers for knock-down confirmation was determined. The amplification worked well for the whole temperature range (50-62°C, data not shown). Therefore, 60°C was chosen for the quantitative PCR experiment.

Real-time PCR was performed in duplicates with the samples from GFP and Salp25D group. Actin served as a reference gene. The obtained values of threshold cycle (C_T) were averaged for each duplicate and used for the relative quantification by comparative C_T method. Data for the analysis are summarized in Table 16. Threshold cycle values for actin amplification were constant as expected for a housekeeping gene. Also, Ct values of duplicate measurements did not differ by more than one cycle, which is a requirement for a confident analysis. The sample with highest expression (GFP-gut) was used as a calibrator to which the other samples were normalized.

Table 16: Analysis of qPCR results by comparative C_T method. The average threshold cycle values (avg. C_T) of Salp25D and GFP group were subtracted. The ΔC_T of individual organs was lowered by the ΔC_T value of the calibrator (GFP-gut). The equation describing the relative gene expression ($2^{-\Delta\Delta CT}$) assumes 100% amplification efficiency. The result is expressed in as % relative expression.

sample	avg. C_T Salp25D	avg. C_T GFP	ΔC_T	$\Delta C_T - \Delta C_{T,cal}$	$2^{-\Delta\Delta CT}$	%
GFP - SG	37,635	30,250	7,385	3,0500	0,121	12,07
SALP25D - SG	40,000	30,275	9,725	5,390	0,024	2,38
GFP - OV	37,695	29,840	7,855	3,520	0,087	8,72
SALP25D - OV	40,000	30,245	9,755	5,420	0,023	2,34
GFP - G	34,885	30,550	4,335	0,000	1,000	100
SALP25D - G	38,345	30,200	8,145	3,810	0,071	7,13

The expression of Salp25D gene was the highest in the gut of GFP control group. After gene silencing by Salp25D dsRNA, the expression dropped dramatically (14 times decreased). The gene silencing was also observed in the other organs, but not to that extent as in the gut. In salivary glands, the expression was diminished 5 times, and in ovaries, 3.7 times (Graph 4), which is still a sign of a successful knock-down.

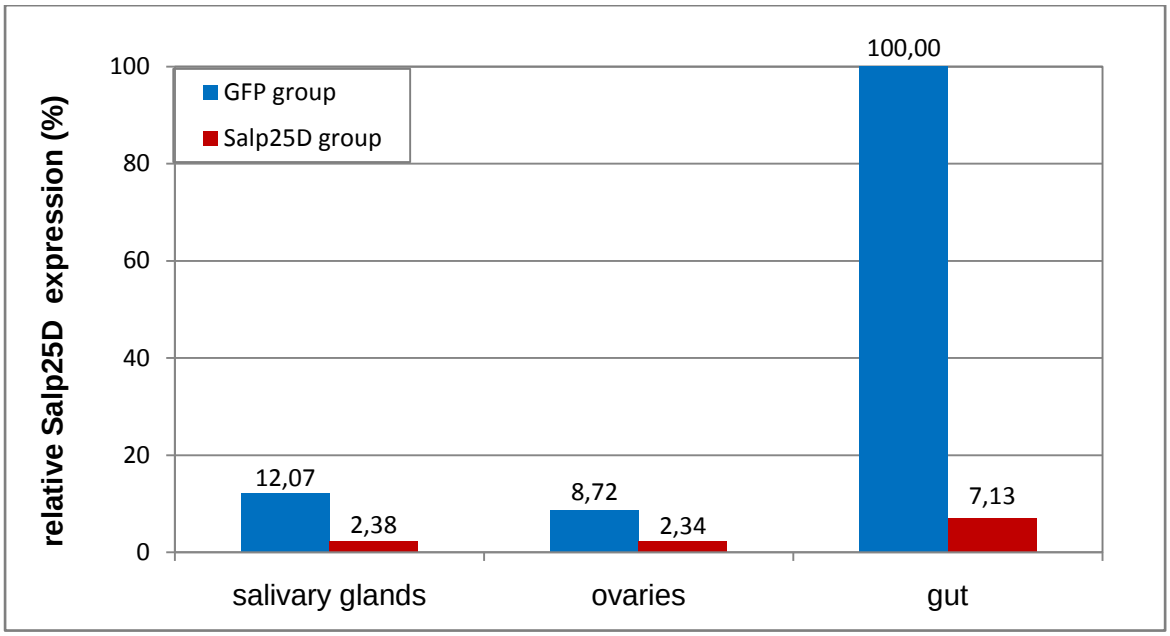

Graph 4: Silencing of Salp25D gene in tick organs. The sample with highest expression (GFP- gut) was used as a calibrator and other values were normalized to it. Blue columns represent the expression of Salp25D in GFP- injected control group; red columns represent the expression of Salp25D in Salp25D-injected group.

6 DISCUSSION AND CONCLUSIONS

Ticks present a thread for their vertebrate hosts as they can transmit various pathogens causing serious infections with potentially fatal consequences. Understanding the tick immune system and the processes underlying their hematophagous lifestyle is an important issue that should be addressed. Characterization of individual tick proteins represents a useful method to accomplish the goal.

We have attempted the molecular and biochemical characterization of a putative antioxidant enzyme from *Ixodes ricinus*, Salp25D. It was named after homologous protein found in *Ixodes scapularis*. The name reflects the fact that it was first identified as a salivary protein with the molecular mass of approximately 25 kDa (*108*).

The *I. ricinus* Salp25D cDNA contains a single open reading frame encoding a 221 amino acid protein. The protein shares a similarity with peroxiredoxins of various species across the phyla, indicating the conservation of these proteins during the evolution. Salp25D shows particularly strong homology with tick antioxidant enzymes (99% identity with *I. scapularis* Salp25D on a protein level, 91% identity with *H. longicornis* peroxiredoxin). For other 1-Cys peroxiredoxins from invertebrate (fruit fly, sea urchin, lugworm) and vertebrate (human, cow, mouse) species, the amino acid sequence similarity is also quite high, mostly exceeding 60%. The peroxidase motif PVCTXE typical for 1-Cys Prxs is conserved in all these proteins.

Stage- and tissue- specific expression profiles of Salp25D were determined. It was revealed, that the gene is expressed in all developmental stages (larvae, nymph, adult) of *I. ricinus*. The expression was observed in both unfed and fed ticks, but it was higher after feeding. Concerning the organ distribution, it was shown that the protein is expressed preferentially in gut, ovaries and salivary glands (*141*). As these organs come into contact with host blood antigens, the expression may be related to tick defense.

The expression in salivary glands was expected, according to previous studies (*83, 108*). However, the bioinformatic search revealed that the hydrophobic signal peptide sequence is missing in the protein (*141*). Such N-terminal peptide is characteristic for secreted salivary proteins. The lack of signal sequence was reported also for other, highly similar, antioxidant enzymes from tick salivary glands (*83, 108*). Since the tick immune host developed

antibodies against these proteins, it was clear that the enzyme has to use some alternative pathway to get into tick saliva. It was suggested that the secretion may occur via cell degradation, cell leakiness, or other mechanism (*83*, *108*).

Besides, high Salp25D expression was found in the tick midgut. This leads us to the hypothesis that the gut Salp25D may be important in processes connected to blood digestion, such as the detoxification of oxygen radicals produced during the heme metabolism. This was already observed for *R. microplus* catalase (*98*).

It seems, the Salp25D plays an important role in the tick gut as well as on the host skin. For *I. scapularis*, it was hypothesized that it may be the salivary Salp25D that provides the advantage to the pathogens in the gut, because some saliva goes to the gut together with host blood during tick feeding (*145*). As proposed for antioxidant enzymes in general (*83*), Salp25D may be implicated in detoxification of its own reactive oxygen species in the tick as well as in the defense against oxidative burst triggered by host immunity. During this process, the neutrophils migrating to the bite site produce oxygen radicals in order to fight the pathogens. For hard ticks, it is of high priority to successfully quench these radicals, because they require a prolonged period of feeding (4-6 days). Therefore, Salp25D from *I. scapularis* and *I. ricinus* may represent one of the potential strategies of evading the host immunity, leading to the successful tick-feeding process (*108*).

Prior to the recent study, the gene for Salp25D was cloned into an expression vector and pilot expression and purification experiments were done. We decided to prepare a recombinant protein in bacterial cells, because it is probably the easiest way to obtain sufficient amounts of a protein. It was shown that the recombinant protein can be purified under native conditions (*141*). This finding was promising, as it provided a good chance for production of an active protein.

The rSalp25D produced in the pilot expression experiments was preliminary tested for the antioxidant activity, but turned to be inactive (*141*). The optimizaton of expression and purification conditions provided in this thesis resulted in increase of the functional activity of the newly prepared rSalp25D.

It has been already shown in several experiments that 1-Cys (*83, 109)* as well as 2-Cys peroxiredoxins (*146–148*) can prevent the formation of harmful hydroxyl radicals and protect supercoiled DNA from single-stranded breaks. *I. scapularis* Salp25D was able to

protect the supercoiled form of plasmid at the concentration of 28 nM (2 μg/ml) concentration (*109)* and the peroxiredoxin from *H. longicornis* at 25 μg/ml (*83).* To test if the *I. ricinus* rSalp25D has also the same ability, we produced hydroxyl radicals *in vitro* by thiol-containing metal-catalyzed reaction. The ability to protect the supercoiled DNA was detected from the concentration of 50 μg/ml of rSalp25D and increased in a dose-dependent manner.

The involvement of tick salivary proteins in facilitation of the acquisition and transmission of *B. burgdorferi* has been described previously (*109*, *125–127*). Antioxidant enzymes were assumed to participate in this process. By their action, they may allow the spirochetes to escape reactive oxygen mediated damage during the acquisition by the vector or transmission to the host. The protection of borrelia from oxidative stress *in vitro* was shown with *I. scapularis* SGE, where the spirochetes incubated with tick SGE survived the treatment with PMA-activated neutrophils (*109*). *In vivo* experiments indicated that salivary *I. scapularis* Salp25D silencing dramatically decreased the acquisition of Borrelia by the tick feeding on infected host. On the other hand, the knockdown did not have a significant effect on Borrelia transmission from the ticks to an uninfected host (*109*).

An experiment was conducted to test if *I. ricinus* Salp25D can protect borrelia from oxidative stress-mediated killing *in vitro*. In the presence of hydroxyl radicals generated by thiol-containing metal-catalyzed reaction, most borrelia did not survive. Addition of rSalp25D to the reaction rescued a significant portion of spirochetes. These results were consistent with the previous findings (*109*).

It was expected that glutathione might serve as an electron donor for the peroxidation catalyzed by *I. ricinus* rSalp25D. The assumption that catalytic activity might be glutathione-dependent was based on the findings of *I. scapularis* Salp25D. There, the recombinant protein exhibited a glutathione peroxidase activity *in vitro* (*108*). However, we can speculate that the activity was achieved by using extremely high concentrations of protein (up to 1 mM), which is not the normal case for enzymes. Also, *I. scapularis* Salp25D was expressed as a fusion protein with thioredoxin. The choice of this particular fusion partner might be the reason, why the enzymatic activity was present in their case.

The fact that purified recombinant or native proteins often tend to lose their GSH peroxidase activity was already noted before and was ascribed to the oxidation of the conserved cysteine residue (*66*). This might be the case of *I. ricinus* rSalp25D as well. However, the literature is

highly inconsistent in the question of redox partners for 1-Cys peroxiredoxins (*41*). As for other proteins of the same type, the physiological partner for Salp25D remains to be elucidated. Utilizing thioredoxin or glutaredoxin electron donors might be the possible option for further studies.

RNA interference is a gene-silencing technique that helps greatly in studying of gene functions. In ticks, it has become a valuable tool for the description of tick-pathogen interface as well as for the screening of tick protective antigens (*146*).

By the injection of dsRNA into the body of the tick, the *I. ricinus* Salp25D gene was knocked down in all organs of *I. ricinus*, with highest efficiency in the tick gut. The study will further focus on phenotypic features of this knockdown, with the emphasis on tick-host-pathogen interaction. The future plans involve the investigation of how the gene silencing affects borrelia acquisition by ticks or their transmission to uninfected host. In addition, due to high expression of Salp25D observed in tick gut, it would be intresting to determine if the Salp25D knock-down impairs detoxification of peroxides in the gut.

The recent research mainly focuses on the proteins that are important in the tick life cycle and feeding process. Salp25D, an antioxidant enzyme, might be the part of this system. Such proteins may be targeted and serve as candidate molecules for the control of ticks as well as tick-borne pathogens (*132*). Since preventing the tick-borne diseases based on the targeting of pathogen antigens turned out to be difficult (*109*), the manipulation of vector antigens may provide a better way how to disrupt the tick life cycle and inhibit the migration of pathogens into the host (*132*, *147*, *148*).

7 BIBLIOGRAPHY

1. Forman, H. J., Maiorino, M., and Ursini, F. (2010) Signaling functions of reactive oxygen species, *Biochemistry 49*, 835–842.
2. Babior, B. M. (2000) Phagocytes and oxidative stress, *Am J Med 109*, 33–44.
3. Valko, M., Rhodes, C. J., Moncol, J., Izakovic, M., and Mazur, M. (2006) Free radicals, metals and antioxidants in oxidative stress-induced cancer, *Chem-Biol Interact 160*, 1–40.
4. Novo, E., and Parola, M. (2008) Redox mechanisms in hepatic chronic wound healing and fibrogenesis, *Fibrogenesis Tissue Repair 1*, 5.
5. Inoue, M., Sato, E. F., Nishikawa, M., Park, A.-M., Kira, Y., Imada, I., and Utsumi, K. (2003) Mitochondrial generation of reactive oxygen species and its role in aerobic life, *Curr Med Chem 10*, 2495–2505.
6. Halliwell, B., and Gutteridge, J. M. C. (1985) Free radicals in biology and medicine, Clarendon Press.
7. Segal, A. W. (2005) How neutrophils kill microbes, *Annu Rev Immunol 23*, 197–223.
8. Pritsos, C. A. (2000) Cellular distribution, metabolism and regulation of the xanthine oxidoreductase enzyme system, *Chem-Biol Interact 129*, 195–208.
9. Finkel, T., and Holbrook, N. J. (2000) Oxidants, oxidative stress and the biology of ageing, *Nature 408*, 239–247.
10. Cooke, M. S., Evans, M. D., Dizdaroglu, M., and Lunec, J. (2003) Oxidative DNA damage: mechanisms, mutation, and disease, *FASEB J 17*, 1195–1214.
11. Cheng, K. C., Cahill, D. S., Kasai, H., Nishimura, S., and Loeb, L. A. (1992) 8-Hydroxyguanine, an abundant form of oxidative DNA damage, causes G->T and A->C substitutions, *J Biol Chem 267*, 166–172.
12. Kohen, R., and Nyska, A. (2002) Oxidation of biological systems: oxidative stress phenomena, antioxidants, redox reactions, and methods for their quantification, *Toxicol Pathol 30*, 620–650.
13. Guéraud, F., Atalay, M., Bresgen, N., Cipak, A., Eckl, P. M., Huc, L., Jouanin, I., Siems, W., and Uchida, K. (2010) Chemistry and biochemistry of lipid peroxidation products, *Free Radic Res 44*, 1098–1124.
14. Marnett, L. J. (1999) Lipid peroxidation-DNA damage by malondialdehyde, *Mutat Res 424*, 83–95.
15. Stadtman, E. R. (2004) Role of oxidant species in aging, *Curr Med Chem 11*, 1105–1112.
16. Zglinicki, T. von. (2003) Aging at the Molecular Level, Springer.
17. Fridovich, I. (2007) ROS-dependent enzymes - Catalase. In *Redox Biochemistry* (Banerjee, R., Ed.), John Wiley & Sons.
18. Wu, A. J., Penner-Hahn, J. E., and Pecoraro, V. L. (2004) Structural, spectroscopic, and reactivity models for the manganese catalases, *Chem Rev 104*, 903–938.
19. Goodsell, D. S. (2007) Superoxide Dismutase, *RCSB Protein Data Bank*.

20. Youn, H. D., Kim, E. J., Roe, J. H., Hah, Y. C., and Kang, S. O. (1996) A novel nickel-containing superoxide dismutase from *Streptomyces* spp., *Biochem J 318*, 889–896.

21. Bryngelson, P. A., and Maroney, M. J. (2007) Nickel superoxide dismutase. In *Nickel and Its Surprising Impact in Nature* (Sigel, A., Sigel, H., and Sigel, R. K. O., Eds.), 417–443, John Wiley & Sons.

22. Toppo, S., Flohé, L., Ursini, F., Vanin, S., and Maiorino, M. (2009) Catalytic mechanisms and specificities of glutathione peroxidases: Variations of a basic scheme, *BBA - Gen Subjects 1790*, 1486–1500.

23. Gladyshev, V. N. (2007) Selenoproteins. In *Redox Biochemistry* (Banerjee, R., Ed.), John Wiley & Sons.

24. Bell, J. G., Cowey, C. B., and Youngson, A. (1984) Rainbow trout liver microsomal lipid peroxidation the effect of purified glutathione peroxidase, glutathione S-transferase and other factors, *BBA - Lipid Lipid Met 795*, 91–99.

25. Maiorino, M., Roche, C., Kiess, M., Koenig, K., Gawlik, D., Matthes, M., Naldini, E., Pierce, R., and Flohé, L. (1996) A selenium-containing phospholipid-hydroperoxide glutathione peroxidase in *Schistosoma mansoni*, *Eur J Biochem 238*, 838–844.

26. Maiorino, M., Ursini, F., Bosello, V., Toppo, S., Tosatto, S. C. E., Mauri, P., Becker, K., Roveri, A., Bulato, C., Benazzi, L., De Palma, A., and Flohé, L. (2007) The Thioredoxin Specificity of *Drosophila* GPx: A paradigm for a peroxiredoxin-like mechanism of many glutathione peroxidases, *J Mol Biol 365*, 1033–1046.

27. Schlecker, T., Comini, M. A., Melchers, J., Ruppert, T., and Krauth-Siegel, R. L. (2007) Catalytic mechanism of the glutathione peroxidase-type tryparedoxin peroxidase of *Trypanosoma brucei*, *Biochem J 405*, 445–454.

28. Tosatto, S. C. E., Bosello, V., Fogolari, F., Mauri, P., Roveri, A., Toppo, S., Flohé, L., Ursini, F., and Maiorino, M. (2008) The catalytic site of glutathione peroxidases, *Antioxid Redox Signal 10*, 1515–1526.

29. Deponte, M. (2012) Glutathione catalysis and the reaction mechanisms of glutathione-dependent enzymes, *Biochim Biophys Acta*. DOI: 10.1016/j.bbagen.2012.09.018

30. Peshenko, I. V., and Shichi, H. (2001) Oxidation of active center cysteine of bovine 1-Cys peroxiredoxin to the cysteine sulfenic acid form by peroxide and peroxynitrite, *Free Radic Biol Med 31*, 292–303.

31. Kumagai, T., Osada, Y., Ohta, N., and Kanazawa, T. (2009) Peroxiredoxin-1 from *Schistosoma japonicum* functions as a scavenger against hydrogen peroxide but not nitric oxide, *Mol Biochem Parasit 164*, 26–31.

32. Bryk, R., Griffin, P., and Nathan, C. (2000) Peroxynitrite reductase activity of bacterial peroxiredoxins, *Nature 407*, 211–215.

33. Trujillo, M., Ferrer-Sueta, G., Thomson, L., Flohé, L., and Radi, R. (2007) Kinetics of peroxiredoxins and their role in the decomposition of peroxynitrite, *Subcell Biochem 44*, 83–113.

34. Wood, Z. A., Schröder, E., Robin Harris, J., and Poole, L. B. (2003) Structure, mechanism and regulation of peroxiredoxins, *Trends Biochem Sci 28*, 32–40.

35. Fisher, A. B. (2011) Peroxiredoxin 6: A bifunctional enzyme with glutathione peroxidase and phospholipase A2 activities, *Antioxid Redox Signal 15*, 831–844.

36. Rhee, S. G., Kang, S. W., Chang, T. S., Jeong, W., and Kim, K. (2001) Peroxiredoxin, a novel family of peroxidases, *IUBMB Life 52*, 35–41.

37. Soito, L., Williamson, C., Knutson, S. T., Fetrow, J. S., Poole, L. B., and Nelson, K. J. (2011) PREX: PeroxiRedoxin classification indEX, a database of subfamily assignments across the diverse peroxiredoxin family, *Nucleic Acids Res 39*, D332–337.

38. Hall, A., Nelson, K., Poole, L. B., and Karplus, P. A. (2011) Structure-based insights into the catalytic power and conformational dexterity of peroxiredoxins, *Antioxid Redox Signal 15*, 795–815.

39. Poole, L. B., Hall, A., and Nelson, K. J. (2011) Overview of peroxiredoxins in oxidant defense and redox regulation. In *Curr Protoc Toxicol* (Bus, J. S., Costa, L. G., Hodgson, E., Lawrence, D. A., and Reed, D. J., Eds.), John Wiley & Sons.

40. Jang, H. H., Lee, K. O., Chi, Y. H., Jung, B. G., Park, S. K., Park, J. H., Lee, J. R., Lee, S. S., Moon, J. C., Yun, J. W., Choi, Y. O., Kim, W. Y., Kang, J. S., Cheong, G.-W., Yun, D.-J., Rhee, S. G., Cho, M. J., and Lee, S. Y. (2004) Two enzymes in one: Two yeast peroxiredoxins display oxidative stress-dependent switching from a peroxidase to a molecular chaperone function, *Cell 117*, 625–635.

41. Manevich, Y., and Fisher, A. B. (2005) Peroxiredoxin 6, a 1-Cys peroxiredoxin, functions in antioxidant defense and lung phospholipid metabolism, *Free Radic Biol Med 38*, 1422–1432.

42. Poole, L. B. (2007) Peroxiredoxins. In *Redox Biochemistry* (Banerjee, R., Ed.), John Wiley & Sons.

43. Hall, A., Parsonage, D., Poole, L. B., and Karplus, P. A. (2010) Structural evidence that peroxiredoxin catalytic power is based on transition-state stabilization, *J Mol Biol 402*, 194–209.

44. Hall, A., Karplus, P. A., and Poole, L. B. (2009) Typical 2-Cys peroxiredoxins: Structures, mechanisms and functions, *FEBS J 276*, 2469–2477.

45. Rhee, S. G., Chae, H. Z., and Kim, K. (2005) Peroxiredoxins: a historical overview and speculative preview of novel mechanisms and emerging concepts in cell signaling, *Free Radic Biol Med 38*, 1543–1552.

46. Veal, E. A., Day, A. M., and Morgan, B. A. (2007) Hydrogen peroxide sensing and signaling, *Mol Cell 26*, 1–14.

47. Chang, T.-S., Jeong, W., Choi, S. Y., Yu, S., Kang, S. W., and Rhee, S. G. (2002) Regulation of peroxiredoxin I activity by Cdc2-mediated phosphorylation, *J Biol Chem 277*, 25370–25376.

48. Kang, S. W., Rhee, S. G., Chang, T.-S., Jeong, W., and Choi, M. H. (2005) 2-Cys peroxiredoxin function in intracellular signal transduction: therapeutic implications, *Trends Mol Med 11*, 571–578.

49. Chae, H. Z., Oubrahim, H., Park, J. W., Rhee, S. G., and Chock, P. B. (2012) Protein glutathionylation in the regulation of peroxiredoxins: a family of thiol-specific peroxidases that function as antioxidants, molecular chaperones, and signal modulators, *Antioxid Redox Signal 16*, 506–523.

50. Moon, J. C., Hah, Y.-S., Kim, W. Y., Jung, B. G., Jang, H. H., Lee, J. R., Kim, S. Y., Lee, Y. M., Jeon, M. G., Kim, C. W., Cho, M. J., and Lee, S. Y. (2005) Oxidative stress-dependent structural and functional switching of a human 2-Cys peroxiredoxin isotype II that enhances HeLa cell resistance to H_2O_2-induced cell death, *J Biol Chem 280*, 28775–28784.

51. Choi, J., Choi, S., Choi, J., Cha, M.-K., Kim, I.-H., and Shin, W. (2003) Crystal structure of *Escherichia coli* thiol peroxidase in the oxidized state: insights into intramolecular disulfide formation and substrate binding in atypical 2-Cys peroxiredoxins, *J Biol Chem 278*, 49478–49486.

52. Knoops, B., Goemaere, J., Van der Eecken, V., and Declercq, J.-P. (2011) Peroxiredoxin 5: structure, mechanism, and function of the mammalian atypical 2-Cys peroxiredoxin, *Antioxid Redox Signal 15*, 817–829.

53. Clarke, D. J., Ortega, X. P., Mackay, C. L., Valvano, M. A., Govan, J. R. W., Campopiano, D. J., Langridge-Smith, P., and Brown, A. R. (2010) Subdivision of the bacterioferritin comigratory protein family of bacterial peroxiredoxins based on catalytic activity, *Biochemistry 49*, 1319–1330.

54. Lu, J., Yang, F., Li, Y., Zhang, X., Xia, B., and Jin, C. (2008) Reversible conformational switch revealed by the redox structures of *Bacillus subtilis* thiol peroxidase, *Biochem Biophys Res Commun 373*, 414–418.

55. Hall, A., Sankaran, B., Poole, L. B., and Karplus, P. A. (2009) Structural changes common to catalysis in the Tpx peroxiredoxin subfamily, *J Mol Biol 393*, 867–881.

56. Rouhier, N., Gelhaye, E., Gualberto, J. M., Jordy, M.-N., Fay, E. D., Hirasawa, M., Duplessis, S., Lemaire, S. D., Frey, P., Martin, F., Manieri, W., Knaff, D. B., and Jacquot, J.-P. (2004) Poplar Peroxiredoxin Q. A thioredoxin-linked chloroplast antioxidant functional in pathogen defense, *Plant Physiol 134*, 1027–1038.

57. Fisher, A. B., Dodia, C., Manevich, Y., Chen, J. W., and Feinstein, S. I. (1999) Phospholipid hydroperoxides are substrates for non-selenium glutathione peroxidase, *J Biol Chem 274*, 21326–21334.

58. Nevalainen, T. J. (2010) 1-Cysteine peroxiredoxin: A dual-function enzyme with peroxidase and acidic Ca^{2+}-independent phospholipase A2 activities, *Biochimie 92*, 638–644.

59. Chen, J.-W., Dodia, C., Feinstein, S. I., Jain, M. K., and Fisher, A. B. (2000) 1-Cys Peroxiredoxin, a bifunctional enzyme with glutathione peroxidase and phospholipase A2 activities, *J Biol Chem 275*, 28421–28427.

60. Kang, S. W., Baines, I. C., and Rhee, S. G. (1998) Characterization of a mammalian peroxiredoxin that contains one conserved cysteine, *J Biol Chem 273*, 6303–6311.

61. Pedrajas, J. R., Miranda-Vizuete, A., Javanmardy, N., Gustafsson, J.-Å., and Spyrou, G. (2000) Mitochondria of *Saccharomyces cerevisiae* contain one-conserved cysteine type peroxiredoxin with thioredoxin peroxidase activity, *J Biol Chem 275*, 16296–16301.

62. Greetham, D., and Grant, C. M. (2009) Antioxidant activity of the yeast mitochondrial one-Cys peroxiredoxin is dependent on thioredoxin reductase and glutathione in vivo, *Mol Cell Biol 29*, 3229–3240.

63. Shichi, H. (1990) Glutathione-dependent detoxification of peroxide in bovine ciliary body, *Exp Eye Res 50*, 813–818.

64. Pérez-Pérez, M. E., Mata-Cabana, A., Sánchez-Riego, A. M., Lindahl, M., and Florencio, F. J. (2009) A comprehensive analysis of the peroxiredoxin reduction system in the Cyanobacterium *Synechocystis* sp. strain PCC 6803 reveals that all five peroxiredoxins are thioredoxin dependent, *J Bacteriol 191*, 7477–7489.

65. Radyuk, S. N., Klichko, V. I., Spinola, B., Sohal, R. S., and Orr, W. C. (2001) The peroxiredoxin gene family in *Drosophila melanogaster*, *Free Radic Biol Med 31*, 1090–1100.

66. Manevich, Y., Feinstein, S. I., and Fisher, A. B. (2004) Activation of the antioxidant enzyme 1-CYS peroxiredoxin requires glutathionylation mediated by heterodimerization with πGST, *PNAS 101*, 3780–3785.

67. Monteiro, G., Horta, B. B., Pimenta, D. C., Augusto, O., and Netto, L. E. S. (2007) Reduction of 1-Cys peroxiredoxins by ascorbate changes the thiol-specific antioxidant paradigm, revealing another function of vitamin C, *PNAS 104*, 4886–4891.

68. Pedrajas, J. R., Padilla, C. A., McDonagh, B., and Bárcena, J. A. (2010) Glutaredoxin participates in the reduction of peroxides by the mitochondrial 1-CYS peroxiredoxin in *Saccharomyces cerevisiae*, *Antioxid Redox Signal 13*, 249–258.

69. Lee, S. P., Hwang, Y. S., Kim, Y. J., Kwon, K. S., Kim, H. J., Kim, K., and Chae, H. Z. (2001) Cyclophilin a binds to peroxiredoxins and activates its peroxidase activity, *J Biol Chem 276*, 29826–29832.

70. Manevich, Y., Reddy, K. S., Shuvaeva, T., Feinstein, S. I., and Fisher, A. B. (2007) Structure and phospholipase function of peroxiredoxin 6: identification of the catalytic triad and its role in phospholipid substrate binding, *J Lipid Res 48*, 2306–2318.

71. Kim, T.-S., Sundaresh, C. S., Feinstein, S. I., Dodia, C., Skach, W. R., Jain, M. K., Nagase, T., Seki, N., Ishikawa, K., Nomura, N., and Fisher, A. B. (1997) Identification of a human cDNA clone for lysosomal type Ca^{2+}-independent phospholipase A2 and properties of the expressed protein, *J Biol Chem 272*, 2542–2550.

72. Kim, T. S., Dodia, C., Chen, X., Hennigan, B. B., Jain, M., Feinstein, S. I., and Fisher, A. B. (1998) Cloning and expression of rat lung acidic Ca(2+)-independent PLA2 and its organ distribution, *Am J Physiol 274*, L750–761.

73. Akiba, S., Dodia, C., Chen, X., and Fisher, A. B. (1998) Characterization of acidic Ca(2+)-independent phospholipase A2 of bovine lung, *Comp Biochem Physiol B, Biochem Mol Biol 120*, 393–404.

74. Holmgren, A. (2007) The thioredoxin system. In *Redox Biochemistry* (Banerjee, R., Ed.), John Wiley & Sons.

75. Lou, M. F. (2007) The glutathione system. In *Redox Biochemistry* (Banerjee, R., Ed.), John Wiley & Sons.

76. Frein, D., Schildknecht, S., Bachschmid, M., and Ullrich, V. (2005) Redox regulation: a new challenge for pharmacology, *Biochem Pharmacol 70*, 811–823.

77. Goddard, J. (2008) Infectious Diseases and Arthropods, Springer.

78. De la Fuente, J., Estrada-Pena, A., Venzal, J. M., Kocan, K. M., and Sonenshine, D. E. (2008) Overview: Ticks as vectors of pathogens that cause disease in humans and animals, *Front Biosci 13*, 6938–6946.

79. Sonenshine, D. E. (1991) Biology of ticks, Oxford University Press.

80. Randolph, S. E. (2001) The shifting landscape of tick-borne zoonoses: tick-borne encephalitis and Lyme borreliosis in Europe, *Phil Trans R Soc Lond B 356*, 1045–1056.

81. Parola, P., and Raoult, D. (2001) Ticks and tickborne bacterial diseases in humans: an emerging infectious threat, *Clin Infect Dis 32*, 897–928.

82. Pereira, L. S., Oliveira, P. L., Barja-Fidalgo, C., and Daffre, S. (2001) Production of reactive oxygen species by hemocytes from the cattle tick *Boophilus microplus*, *Exp Parasitol 99*, 66–72.

83. Tsuji, N., Kamio, T., Isobe, T., and Fujisaki, K. (2001) Molecular characterization of a peroxiredoxin from the hard tick *Haemaphysalis longicornis*, *Insect Mol Biol 10*, 121–129.

84. Balashov, Y. S. (1972) Bloodsucking ticks (Ixodoidea)-vectors of diseases of man and animals. Entomological Society of America.

85. Graça-Souza, A. V., Maya-Monteiro, C., Paiva-Silva, G. O., Braz, G. R. C., Paes, M. C., Sorgine, M. H. F., Oliveira, M. F., and Oliveira, P. L. (2006) Adaptations against heme toxicity in blood-feeding arthropods, *Insect Biochem Mol Biol 36*, 322–335.

86. Toh, S. Q., Glanfield, A., Gobert, G. N., and Jones, M. K. (2010) Heme and blood-feeding parasites: friends or foes?, *Parasit Vectors 3*, 108.

87. Schmitt, T. H., Frezzatti, W. A., and Schreier, S. (1993) Hemin-induced lipid membrane disorder and increased permeability: A molecular model for the mechanism of cell lysis, *Archives of Biochem Biophys 307*, 96–103.

88. Gutteridge, J. M., and Smith, A. (1988) Antioxidant protection by haemopexin of haem-stimulated lipid peroxidation., *Biochem J 256*, 861–865.

89. Van Der Zee, J., Barr, D. P., and Mason, R. P. (1996) ESR spin trapping investigation of radical formation from the reaction between hematin and tert-butyl hydroperoxide, *Free Radic Biol Med 20*, 199–206.

90. Sadrzadeh, S., Graf, E., Panter, S., Hallaway, P., and Eaton, J. (1984) Hemoglobin. A biologic fenton reagent, *J Biol Chem 259*, 14354–14356.

91. Ryter, S. W., and Tyrrell, R. M. (2000) The heme synthesis and degradation pathways: role in oxidant sensitivity. Heme oxygenase has both pro- and antioxidant properties, *Free Radic Biol Med 28*, 289–309.

92. Lara, F. A., Lins, U., Paiva-Silva, G., Almeida, I. C., Braga, C. M., Miguens, F. C., Oliveira, P. L., and Dansa-Petretski, M. (2003) A new intracellular pathway of haem detoxification in the midgut of the cattle tick *Boophilus microplus*: aggregation inside a specialized organelle, the hemosome, *J Exp Biol 206*, 1707–1715.

93. Lara, F. A., Lins, U., Bechara, G. H., and Oliveira, P. L. (2005) Tracing heme in a living cell: hemoglobin degradation and heme traffic in digest cells of the cattle tick *Boophilus microplus*, *J Exp Biol 208*, 3093–3101.

94. Maya-Monteiro, C. M., Alves, L. R., Pinhal, N., Abdalla, D. S. P., and Oliveira, P. L. (2004) HeLp, a heme-transporting lipoprotein with an antioxidant role, *Insect Biochem Mol Biol 34*, 81–88.

95. Gudderra, N. P., Neese, P. A., Sonenshine, D. E., Apperson, C. S., and Roe, R. M. (2001) Developmental profile, isolation, and biochemical characterization of a novel lipoglycoheme-carrier protein from the American dog tick, *Dermacentor variabilis* (Acari: Ixodidae) and observations on a similar protein in the soft tick, *Ornithodoros parkeri* (Acari: Argasidae), *Insect Biochem Mol Biol 31*, 299–311.

96. Dupejova, J., Sterba, J., Vancova, M., and Grubhoffer, L. (2011) Hemelipoglycoprotein from the ornate sheep tick, *Dermacentor marginatus*: structural and functional characterization, *Parasit Vectors 4*, 4.

97. Kikuchi, G., Yoshida, T., and Noguchi, M. (2005) Heme oxygenase and heme degradation, *Biochem Biophys Res Comm 338*, 558–567.

98. Citelli, M., Lara, F. A., Da Silva Vaz, I., Jr, and Oliveira, P. L. (2007) Oxidative stress impairs heme detoxification in the midgut of the cattle tick, *Rhipicephalus* (*Boophilus*) *microplus*, *Mol Biochem Parasitol 151*, 81–88.

99. Ribeiro, J. M. C., and Francischetti, I. M. B. (2003) Role of arthropod saliva in blood feeding: sialome and post-sialome perspectives, *Annu Rev Entomol 48*, 73–88.

100. Sanders, H. R., Evans, A. M., Ross, L. S., and Gill, S. S. (2003) Blood meal induces global changes in midgut gene expression in the disease vector, *Aedes aegypti*, *Insect Biochem Mol Biol 33*, 1105–1122.

101. Paes, M. C., Oliveira, M. B., and Oliveira, P. L. (2001) Hydrogen peroxide detoxification in the midgut of the blood-sucking insect, *Rhodnius prolixus*, *Arch Insect Biochem Physiol 48*, 63–71.

102. Magalhaes, T., Brackney, D. E., Beier, J. C., and Foy, B. D. (2008) Silencing an *Anopheles gambiae* catalase and sulfhydryl oxidase increases mosquito mortality after a blood meal, *Arch Insect Biochem Physiol 68*, 134–143.

103. Diaz-Albiter, H., Mitford, R., Genta, F. A., Sant'Anna, M. R. V., and Dillon, R. J. (2011) Reactive oxygen species scavenging by catalase is important for female *Lutzomyia longipalpis* fecundity and mortality, *PLoS One 6*.

104. Kovář, L. (2004) Tick saliva in anti-tick immunity and pathogen transmission, *Folia Microbiol 49*, 327–336.

105. Fontaine, A., Diouf, I., Bakkali, N., Missé, D., Pagès, F., Fusai, T., Rogier, C., and Almeras, L. (2011) Implication of haematophagous arthropod salivary proteins in host-vector interactions, *Parasite Vector 4*, 187.

106. Narasimhan, S., DePonte, K., Marcantonio, N., Liang, X., Royce, T. E., Nelson, K. F., Booth, C. J., Koski, B., Anderson, J. F., Kantor, F., and Fikrig, E. (2007) Immunity against *Ixodes scapularis* salivary proteins expressed within 24 hours of attachment thwarts tick feeding and impairs borrelia transmission, *PLoS ONE 2*, 451.

107. Steiling, H., Munz, B., Werner, S., and Brauchle, M. (1999) Different types of ROS-scavenging enzymes are expressed during cutaneous wound repair, *Exp Cell Res 247*, 484–494.

108. Das, S., Banerjee, G., DePonte, K., Marcantonio, N., Kantor, F. S., and Fikrig, E. (2001) Salp25D, an *Ixodes scapularis* antioxidant, is 1 of 14 immunodominant antigens in engorged tick salivary glands, *J Infect Dis 184*, 1056–1064.

109. Narasimhan, S., Sukumaran, B., Bozdogan, U., Thomas, V., Liang, X., DePonte, K., Marcantonio, N., Koski, R. A., Anderson, J. F., Kantor, F., and Fikrig, E. (2007) A tick antioxidant facilitates the Lyme disease agent's successful migration from the mammalian host to the arthropod vector, *Cell Host Microbe 2*, 7–18.

110. Chang, J. W., Lee, S. H., Lu, Y., and Yoo, Y. J. (2006) Transforming growth factor-β1 induces the non-classical secretion of peroxiredoxin-I in A549 cells, *Biochem Biophys Res Comm 345*, 118–123.

111. Nuttall, P. A., and Labuda, M. (2004) Tick-host interactions: saliva-activated transmission, *Parasitology 129 Suppl*, S177–189.

112. Jones, L. D., Matthewson, M., and Nuttall, P. A. (1992) Saliva-activated transmission (SAT) of Thogoto virus: dynamics of SAT factor activity in the salivary glands of *Rhipicephalus appendiculatus*, *Amblyomma variegatum*, and *Boophilus microplus* ticks, *Exp Appl Acarol 13*, 241–248.

113. Labuda, M., Jones, L. D., Williams, T., and Nuttall, P. A. (1993) Enhancement of tick-borne encephalitis virus transmission by tick salivary gland extracts, *Med Vet Entomol 7*, 193–196.

114. Pechová, J., Štěpánová, G., Kovář, L., and Kopecký, J. (2002) Tick salivary gland extract-activated transmission of *Borrelia afzelii* spirochaetes, *Folia Parasitol 49*, 153–159.

115. Zeidner, N. S., Schneider, B. S., Nuncio, M. S., Gern, L., and Piesman, J. (2002) Coinoculation of *Borrelia* spp. with tick salivary gland lysate enhances spirochete load in mice and is tick species-specific, *J Parasitol 88*, 1276–1278.

116. Lawrie, C. H., Uzcátegui, N. Y., Gould, E. A., and Nuttall, P. A. (2004) Ixodid and argasid tick species and west nile virus, *Emerging Infect Dis 10*, 653–657.

117. Jones, L. D., Davies, C. R., Williams, T., Cory, J., and Nuttall, P. A. (1990) Non-viraemic transmission of Thogoto virus: vector efficiency of *Rhipicephalus appendiculatus* and *Amblyomma variegatum*, *Trans R Soc Trop Med Hyg 84*, 846–848.

118. Richter, D., Allgöwer, R., and Matuschka, F.-R. (2002) Co-feeding transmission and its contribution to the perpetuation of the lyme disease spirochete *Borrelia afzelii*, *Emerging Infect Dis 8*, 1421–1425.

119. Krocová, Z., Macela, A., Hernychová, L., Kroca, M., Pechová, J., and Kopecký, J. (2003) Tick salivary gland extract accelerates proliferation of *Francisella tularensis* in the host, *J Parasitol 89*, 14–20.

120. Lima, C. M. R., Zeidner, N. S., Beard, C. B., Soares, C. A. G., Dolan, M. C., Dietrich, G., and Piesman, J. (2005) Differential infectivity of the Lyme disease spirochete *Borrelia burgdorferi* derived from *Ixodes scapularis* salivary glands and midgut, *J Med Entomol 42*, 506–510.

121. Kýčková, K., and Kopecký, J. (2006) Effect of tick saliva on mechanisms of innate immune response against *Borrelia afzelii*, *J Med Entomol 43*, 1208–1214.

122. Macháčková, M., Oborník, M., and Kopecký, J. (2006) Effect of salivary gland extract from *Ixodes ricinus* ticks on the proliferation of *Borrelia burgdorferi* sensu stricto *in vivo*, *Folia Parasitol 53*, 153–158.

123. Rudolf, I., and Hubálek, Z. (2003) Effect of the salivary gland and midgut extracts from *Ixodes ricinus* and *Dermacentor reticulatus* (Acari: Ixodidae) on the growth of *Borrelia garinii in vitro*, *Folia Parasitol 50*, 159–160.

124. Kuthejlová, M., Kopecký, J., Štěpánová, G., and Macela, A. (2001) Tick salivary gland extract inhibits killing of *Borrelia afzelii* spirochetes by mouse macrophages, *Infect Immun 69*, 575–578.

125. Ramamoorthi, N., Narasimhan, S., Pal, U., Bao, F., Yang, X. F., Fish, D., Anguita, J., Norgard, M. V., Kantor, F. S., Anderson, J. F., Koski, R. A., and Fikrig, E. (2005) The Lyme disease agent exploits a tick protein to infect the mammalian host, *Nature 436*, 573–577.

126. Valenzuela, J. G., Charlab, R., Mather, T. N., and Ribeiro, J. M. (2000) Purification, cloning, and expression of a novel salivary anticomplement protein from the tick, *Ixodes scapularis*, *J Biol Chem 275*, 18717–18723.

127. Tyson, K., Elkins, C., Patterson, H., Fikrig, E., and De Silva, A. (2007) Biochemical and functional characterization of Salp20, an *Ixodes scapularis* tick salivary protein that inhibits the complement pathway, *Insect Mol Biol 16*, 469–479.

128. Wikel, S. K. (1996) Host immunity to ticks, *Annu Rev Entomol 41*, 1–22.

129. Wikel, S. K. (1999) Tick modulation of host immunity: an important factor in pathogen transmission, *Int J Parasit 29*, 851–859.

130. Nazario, S., Das, S., De Silva, A. M., Deponte, K., Marcantonio, N., Anderson, J. F., Fish, D., Fikrig, E., and Kantor, F. S. (1998) Prevention of *Borrelia burgdorferi* transmission in guinea pigs by tick immunity, *Am J Trop Med Hyg 58*, 780–785.

131. Titus, R. G., Bishop, J. V., and Mejia, J. S. (2006) The immunomodulatory factors of arthropod saliva and the potential for these factors to serve as vaccine targets to prevent pathogen transmission, *Parasite Immunol 28*, 131–141.

132. De La Fuente, J., and Kocan, K. M. (2006) Strategies for development of vaccines for control of ixodid tick species, *Parasite Immunol 28*, 275–283.

133. De la Fuente, J., Rodríguez, M., Montero, C., Redondo, M., García-García, J. C., Méndez, L., Serrano, E., Valdés, M., Enríquez, A., Canales, M., Ramos, E., Boué, O., Machado, H., and Lleonart, R. (1999) Vaccination against ticks (*Boophilus* spp.): the experience with the Bm86-based vaccine Gavac, *Genet Anal 15*, 143–148.

134. Trimnell, A. R., Davies, G. M., Lissina, O., Hails, R. S., and Nuttall, P. A. (2005) A cross-reactive tick cement antigen is a candidate broad-spectrum tick vaccine, *Vaccine 23*, 4329–4341.

135. Almazán, C., Kocan, K. M., Blouin, E. F., and De la Fuente, J. (2005) Vaccination with recombinant tick antigens for the control of *Ixodes scapularis* adult infestations, *Vaccine 23*, 5294–5298.

136. Imamura, S., Da Silva Vaz Junior, I., Sugino, M., Ohashi, K., and Onuma, M. (2005) A serine protease inhibitor (serpin) from *Haemaphysalis longicornis* as an anti-tick vaccine, *Vaccine 23*, 1301–1311.

137. Hajdušek, O., Almazán, C., Loosová, G., Villar, M., Canales, M., Grubhoffer, L., Kopáček, P., and De la Fuente, J. (2010) Characterization of ferritin 2 for the control of tick infestations, *Vaccine 28*, 2993–2998.

138. Dai, J., Wang, P., Adusumilli, S., Booth, C. J., Narasimhan, S., Anguita, J., and Fikrig, E. (2009) Antibodies against a tick protein, Salp15, protect mice from the Lyme disease agent, *Cell Host Microbe 6*, 482–492.

139. Kotsyfakis, M., Anderson, J. M., Andersen, J. F., Calvo, E., Francischetti, I. M. B., Mather, T. N., Valenzuela, J. G., and Ribeiro, J. M. C. (2008) Cutting edge: Immunity against a "silent" salivary antigen of the Lyme vector *Ixodes scapularis* impairs its ability to feed, *J Immunol 181*, 5209–5212.

140. Ullmann, A. J., Dolan, M. C., Sackal, C. A., Fikrig, E., Piesman, J., and Zeidner, N. S. Immunization with adenoviral-vectored tick salivary gland proteins (SALPs) in a murine model of Lyme borreliosis, *Ticks Tick Borne Dis*. DOI: 10.1016/j.ttbdis.2012.08.006

141. Jedličková, L. (2009) Izolace a analýza genu Salp25D, homologu glutathion-peroxidázy, klíštěte obecného *Ixodes ricinus*.[Isolation and analysis of Salp25D gene, a homologue of glutathionperoxidase, of the hard tick *Ixodes ricinus*. Bachelor Thesis, in Czech.] - 39 p., Faculty of Science, University of South Bohemia, České Budějovice, Czech Republic.

142. Levashina, E. A., Moita, L. F., Blandin, S., Vriend, G., Lagueux, M., and Kafatos, F. C. (2001) Conserved role of a complement-like protein in phagocytosis revealed by dsRNA knockout in cultured cells of the mosquito, *Anopheles gambiae*, *Cell 104*, 709–718.

143. Netto, L. E., and Stadtman, E. R. (1996) The iron-catalyzed oxidation of dithiothreitol is a biphasic process: hydrogen peroxide is involved in the initiation of a free radical chain of reactions, *Arch Biochem Biophys 333*, 233–242.

144. Lim, Y. S., Cha, M. K., Kim, H. K., Uhm, T. B., Park, J. W., Kim, K., and Kim, I. H. (1993) Removals of hydrogen peroxide and hydroxyl radical by thiol-specific antioxidant protein as a possible role in vivo, *Biochem Biophys Res Commun 192*, 273–280.

145. Anderson, J. M., and Valenzuela, J. G. (2007) Spit-acular entry: Borrelia gets help from a tick salivary protein to move from the mammalian host to the arthropod vector, *Cell Host Microbe 2*, 3–4.

146. De la Fuente, J., Kocan, K. M., Almazán, C., and Blouin, E. F. (2007) RNA interference for the study and genetic manipulation of ticks, *Trends Parasitol 23*, 427–433.

147. Trimnell, A. R., Hails, R. S., and Nuttall, P. A. (2002) Dual action ectoparasite vaccine targeting "exposed" and "concealed" antigens, *Vaccine 20*, 3560–3568.

148. Willadsen, P. (1997) Novel vaccines for ectoparasites, *Vet Parasitol 71*, 209–222.

8 APPENDIX

```
I.ricinus(Salp25D) ----------------------------------MGPLNLGDPFPNFTCDTTEGKIDFHE 26
I.scapularis       ----------------------------------MGPLNLGDPFPNFTCDTTEGKIDFHE 26
A.maculatum        KGVCFDAHGVVFKLSSRKVYTASAERLPTEKRSKMPPLNLGDPFPNFTCDTTVGTIDFHE 60
H.longicornis      ----------------------------------MPPLNLGDPFPNFTCETTVGTIDFHQ 26
O.parkeri          ------------------------------------------------------------
consensus

I.ricinus(Salp25D) WLGNSWGILFSHPADYT-PVCTSELARAAQLHHVFQKKGVKLIALSCDSVESHRGWIKDI 85
I.scapularis       WLGNSWGILFSHPADYT-PVCTSELARAAQLHHVFQKKGVKLIALSCDSVESHRGWIKDI 85
A.maculatum        WLGNSWAILFSHPADYT-PVCTTELARAAQLAHVFEEKGVKLIALSCDSVESHHGWIKDI 119
H.longicornis      WLGDSWGILFSHPADYTTPVCTTELARAAQLAHVFAQKGVKIIALSCDSVDSHHGWIKDI 86
O.parkeri          ----SWGILFSHPADYT-PVCTTELARAAQLAGTFEKKGVKLIALSCDSVDSHKGWIKDI 55
consensus              **.********** ****:********  .* :****:********:**:******

I.ricinus(Salp25D) NAFGELPDGPFPYPIIADEKRDIAVKLGMLDPVEKDKEGLPLTCRAVFIIGPDKKMKLSM 145
I.scapularis       NAFGELPDGPFPYPIIADEKRDIAVKLGMLDPVEKDKEGLPLTCRAVFIIGPDKKMKLSM 145
A.maculatum        EAFGELPDGPFPYPIIADEKREIAVQLGMLDPVEKDKEGLPLTCRAVFIIGPDKKMKLSM 179
H.longicornis      EAFGELPDGPFPYPIIADEKREIAVKLGMLDPVEKDKEGLPLTCRAVFIIGPDKKMKLSM 146
O.parkeri          EAFGELPDGPFPYPIIADEKREIAVELGMLDPVEKDKEGLPLTCRAVFIIGPDKKMKLSM 115
consensus          :*********************:***:********************************

I.ricinus(Salp25D) LYPATTGRNFDEVLRATDSLLVTETRKVATPAGWQKGTPCMVLPSVTEEEIPKLFPTGIK 205
I.scapularis       LYPATTGRNFDEVLRATDSLLVTETRKVATPAGWQKGTPCMVLPSVTEEEILKLFPTGIK 205
A.maculatum        LYPATTGRNFDEVLRATDSLLVTETRKVATPAGWKKGTPCMVLPTVTDEEIPKLFPTGIK 239
H.longicornis      LYPATTGRNFDEVLRATDSLLVTETRKVATPAGWKKGTPCMVLPSVTEEEIPKLFPTGIK 206
O.parkeri          LYPATTGRNFDEVLRATDSLLVTETRKVATPAGWKKGTPCMVLSSVTDEEIPKLFPTGIK 175
consensus          ***********************************:******** :**:*** ********

I.ricinus(Salp25D) QYEVPSGKNYLRTTMD 221
I.scapularis       QYEVPSGKNYLRTTMD 221
A.maculatum        EYPVPSGKKYLRTTMD 255
H.longicornis      QYDVPSGKKYLRTTMD 222
O.parkeri          EIPVPSGKKYLRTTMD 191
consensus          :  *****:*******
```

A: Multiple sequence alignment of known tick 1-cys peroxiredoxins. The alignment was generated using the program ClustalΩ with default settings (http://www.ebi.ac.uk/Tools/msa/clustalo/). Swiss-Prot numbers of aligned sequences: *Ixodes ricinus*- B6V3B5, *Ixodes scapularis*- Q95WZ7, *Amblyomma maculatum*- G3MP44, *Haemaphysalis longicornis*- Q9GV35, *Ornithodoros parkeri*- A6NA14 (truncated protein). Active site cysteine residue is marked red and PVCTXE conserved motif is marked blue. Residues participating at the active site that are conserved in all Prx are green-coloured.

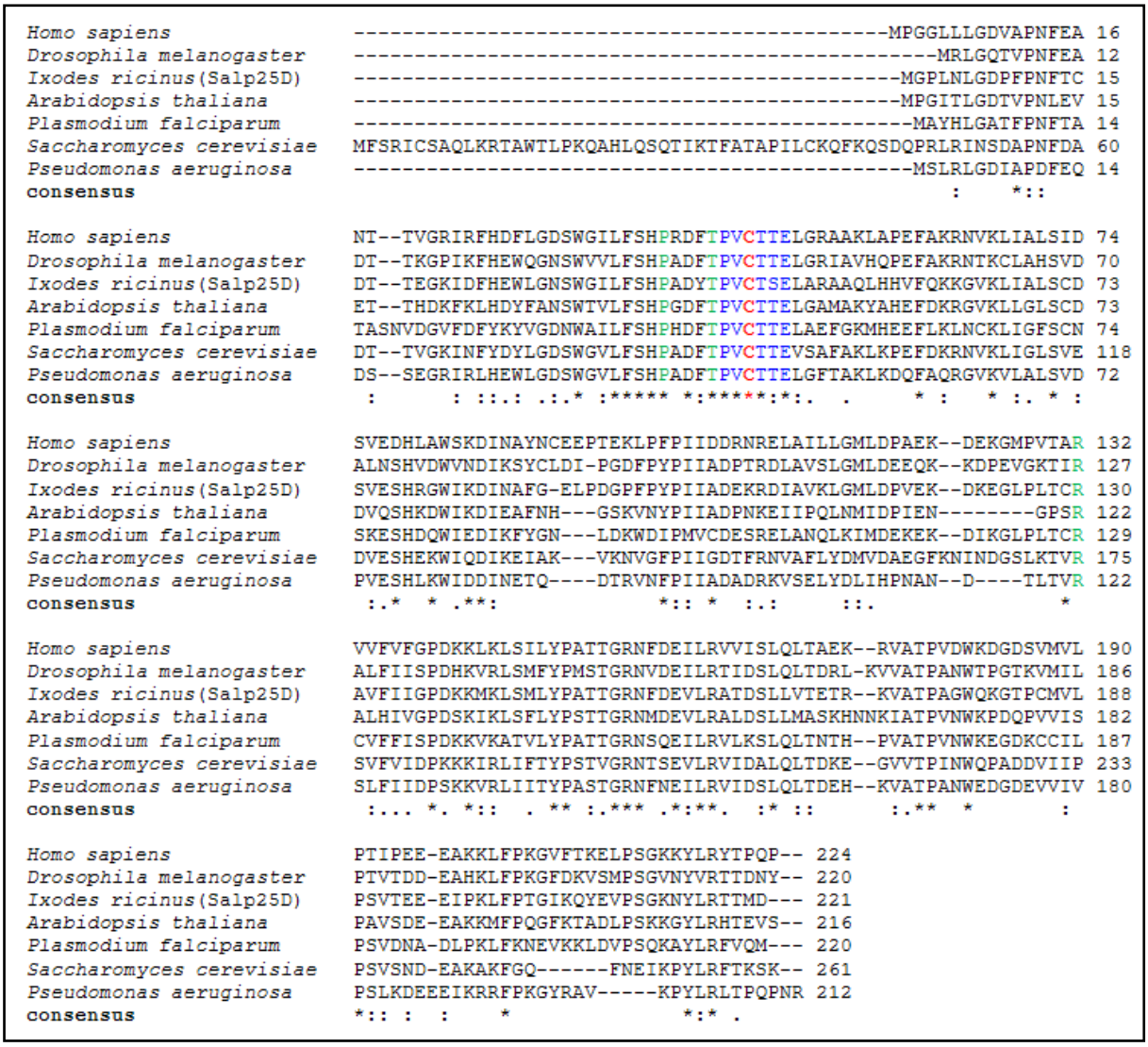

B: Multiple sequence alignment of 1-cys peroxiredoxins from different organisms. The alignment was generated using the program ClustalΩ with default settings (http://www.ebi.ac.uk/Tools/msa/clustalo/). Swiss-Prot numbers of aligned sequences: *Homo sapiens*- P30041, *Drosophila melanogaster*- Q9GPQ0, *Ixodes ricinus*- B6V3B5, *Arabidopsis thaliana*- O04005, *Plasmodium falciparum*- Q9XXW9, *Saccharomyces cerevisiae*- P34227, *Pseudomonas aeruginosa*- Q9HYF6. Active site cysteine residue is marked red and PVCTXE conserved motif is marked blue. Residues participating at the active site that are conserved in all Prx are green-coloured.